AN EXPERIMENTAL INVESTIGATION OF THE VAPOR EXPLOSION PHENOMENA USING A MOLTEN-METAL JET INJECTED INTO DISTILLED WATER

A Dissertation

Presented to

The Faculty of the Department of Mechanical Engineering

University of Houston

In Partial Fulfillment

of the Requirements for the Degree

Doctor of Philosophy

---

by

Raymond Henry Bradley

May 1971

592493

ACKNOWLEDGEMENTS

I would like to express my appreciation to all who have assisted me during the course of this investigation.

The technical support and financial assistance from the National Aeronautics and Space Administration and, in particular, the individuals at the Manned Spacecraft Center have been invaluable.

I am indebted to many of the staff at the University of Houston for their consultation and technical support, especially Dr. Pat Hedgecoxe, Dr. J. E. Cox, J. W. Stevens, and the fellows in the engineering shops. My special thanks goes to Dr. L. C. Witte who served as my dissertation advisor. He has unselfishly contributed his encouragement, professional knowledge, and assistance throughout this effort.

Finally, I would like to thank my wife, Mitzi, for her understanding and many sacrifices that were necessary to make this dissertation possible.

AN EXPERIMENTAL INVESTIGATION OF THE VAPOR EXPLOSION PHENOMENA USING A MOLTEN-METAL JET INJECTED INTO DISTILLED WATER

An Abstract of A Dissertation

Presented to

The Faculty of the Department of Mechanical Engineering

University of Houston

In Partial Fulfillment

of the Requirements for the Degree

Doctor of Philosophy

---

by

Raymond Henry Bradley

May 1971

ABSTRACT

A small diameter jet of molten metal was injected horizontally into a tank of distilled water, which acted as the quenching fluid. The four types of metal that were used as samples were mercury, Asarcolo 158 (a low-melting-temperature fusible alloy), an alloy consisting of 50-percent lead and 50-percent tin, and tin. The investigation demonstrated that neither a solidified shell nor vapor generation is necessary for a so called "vapor explosion" to occur. An unpublished theory that thermal shock is the causative mechanism of the "vapor explosion" is presented along with supporting evidence in this dissertation.

CONTENTS

LIST OF TABLES

LIST OF FIGURES

1. INTRODUCTION

When a molten metal comes into contact with a quenching fluid a violent explosion can occur. This so-called "vapor explosion" is a well known but little understood phenomena. A vapor explosion is an event that is characterized by fragmentation and sudden energy conversion and a subsequent pressure wave. The violence, or magnitude, of such an explosion depends on the quantity and rate of energy release. Witte, et al [1]* have documented several cases whereas both lives and property were lost when a molten metal was allowed to come into contact with a quenching fluid or even a wet surface. The mechanism that triggers the explosion is not known; however, two basic facts have been established. First, the causative mechanism is not due to chemical reaction [2], and second, fragmentation of the sample material is involved. Both experimental results and analyses [3] have shown that the heat transfer rates required to release the observed energy from a smooth metal sample are several orders of magnitude higher than the maximum rates that can be obtained in a laboratory. Thus, it has been concluded that fragmentation of the sample is required to generate the observed explosion violence.

PURPOSE

The purpose of the experimental investigation described herein was to investigate the vapor explosion phenomena and, in particular,

---

* Numbers in brackets refer to references listed at the end of this dissertation.

the causative mechanism. Since fragmentation is required to perpetuate the explosive action, it appears that the mechanism in question is the same mechanism that causes the fragmentation of the sample. Several theories have been presented regarding the mechanism that initiates the explosion. These theories are discussed by Witte et al [1] and are combined and summarized subsequently.

1. The shrinking shell theory proposes that the sample solidifies on the surface and that the solid shell thus formed shrinks which increases the pressure in the sample's molten interior. This pressure increase causes an explosive rupture of the solidified shell.

2. The liquid entrapment theory proposes that quenching fluid is trapped between the sample and a solid surface and the resulting rapid evaporation of the entrapped liquid causes the sample to rupture.

3. The liquid entrainment theory proposes that quenching fluid is drawn into the interior of the sample and the resulting rapid evaporation causes the sample to rupture.

4. The nucleate boiling theory proposes that violent nucleate boiling overcomes the surface tension forces and thus the sample ruptures.

APPROACH

The experimental investigation was conducted by injecting a small-diameter (1/16 inch), jet of molten metal horizontally into a distilled water quenching fluid. This technique for creating a vapor explosion was selected for two reasons. First, it represents a realistic situation whereas molten material may be rapidly injected into a quenching

fluid, such as apparently was the case with the SPERT 1-D reactor explosion [4]; second, this technique eliminates many of the problems encountered in past experimental programs. The majority of the experimental efforts dealing with the vapor-explosion phenomena have been conducted by dropping molten samples into a quenching fluid, usually water. The single sample is photographed and either explodes or does not explode. The exact configuration of the sample is not fixed. The shape varies among experiments and also varies within a single experiment due to distortion from contact with the quenching fluid. The pressure on the sample changes as it penetrates the quenching fluid, and finally, the surface temperature of the sample changes in the air prior to submersion in the quenching liquid.

The use of a small jet for the initiation of a vapor explosion offers several advantages.

1. Known, repeatable sample configuration
2. Constant sample velocity, pressure, and surface temperature
3. Continuous flow until an explosion occurs

A series of experiments was designed using several low-melting-point material and covering a range of injection temperatures. The temperatures and materials were selected to provide data at or near the conditions of explosion onset and hopefully to provide information directly relatable to the basic theories of the cause of vapor explosions.

2. METAL SAMPLES USED IN THE EXPERIMENT

Four types of metal were selected for use in this investigation. The four metals were mercury, a low-melting-temperature fusible alloy, a lead-tin alloy, and tin.

MERCURY

Mercury was used for both equipment development testing and operational firing runs. A certified-analysis high-purity instrument-grade mercury was used throughout the experiment. The degree of purity was indicated on the mercury-container label, which stated, "ANALYSIS: 2,000 grams of mercury completely evaporated quietly at low temperature under vacuum. Allowable residue: 1 part in 10 million. This test is more sensitive than the A.C.S. which requires evaporation of 20 grams."

Mercury was chosen for use in the experiment because of its availability, its room-temperature liquid properties, and its high reflectivity, which would enable higher quality photographs of experimental phenomena to be made. With respect to the room-temperature properties of mercury, it was hoped that vapor-explosion-phenomena theories, which relate to the formation of solid shells after molten-metal cooling, could be checked.

ASARCOLO 158

A series of operational firing runs was made using a low-melting-temperature, eutectic, fusible, alloy, which has the trade-name designation Asarcolo 158. The alloy is similar to the better known Wood's metal and has the following composition.

Element	Percent by weight
Bismuth	50.0
Lead	26.7
Tin	13.3
Cadmium	10.0

Asarcolo 158 was selected for use in the experiment for two primary reasons. It has a low melting point (158°F), and it experiences a small volume change during solidification (less than 1.7 percent). These characteristics of the alloy were felt to have particular importance in the testing of the current theories of the causative mechanisms of the vapor-explosion phenomenon. The thermophysical properties of Asarcolo 158 are given in reference 5.

LEAD-TIN ALLOY

A lead-tin alloy was used for a series of experiment operational firing runs. The alloy, which consisted of 50% Pb - 50% Sn by weight, was selected for use in the experiment primarily because of its ductility characteristics and its low melting point. Both the ductility and the melting-point characteristics of the alloy are considerably better, for the purpose of this experiment, than are those characteristics of either parent metal. In addition, the oxidation characteristics of the lead-tin alloy are also better, for the purposes of this experiment, than are the oxidation characteristics of either parent metal. The lead-tin alloy used throughout the experiment was a high-grade commercial solder, manufactured by the National Lead Company.

TIN

Tin was used for the final series of experiment operational firing runs. Tin was selected for use in the experiment because it had been widely used by other investigators as a drop-test sample in the study of the vapor-explosion phenomena, and because it is known to be highly explosive when dropped into a quenching fluid. The granular, analytical reagent-grade tin that was used throughout the experiment has the following maximum impurity limits.

Element	Percent by weight
Arsenic	0.0001
Carbon	.005
Copper	.001
Iron	.005
Lead	.005
Sulfur	.002
Zinc	.005

3. EQUIPMENT DESCRIPTION

The equipment used in this experiment to study molten-metal jets injected into a quenching fluid was not all available from commercial sources. In general terms, the equipment consisted of a tank containing the quenching fluid, the molten-metal injection apparatus, and the data-collection equipment. The complete set-up is shown in figure 1.

The basic system requirements used in the development of the apparatus were as follows:

1. Prevent contamination of the metal sample and quenching fluid by maximum use of stainless steel in the design of the apparatus.

2. Establish and maintain an inert atmosphere around the sample, with argon as the purging and pressurizing gas.

3. Provide a quick-opening valve and nozzle system that allows minimum jet distortion and temperature stratification.

Standard laboratory equipment was adequate for most aspects of the experiment data collection. However, the frequency and amplitude of the pressure pulses were found to be considerably larger than had been expected, and no recording equipment with the required frequency and amplitude response capabilities was available.

QUENCHING-FLUID TANK

The quenching-fluid tank serves as the container for the quenching fluid and as the structural mount for the molten-metal jet-injector apparatus. The tank is 8 inches wide on each side and is 12 inches high. The top of the tank remains open to the atmosphere throughout

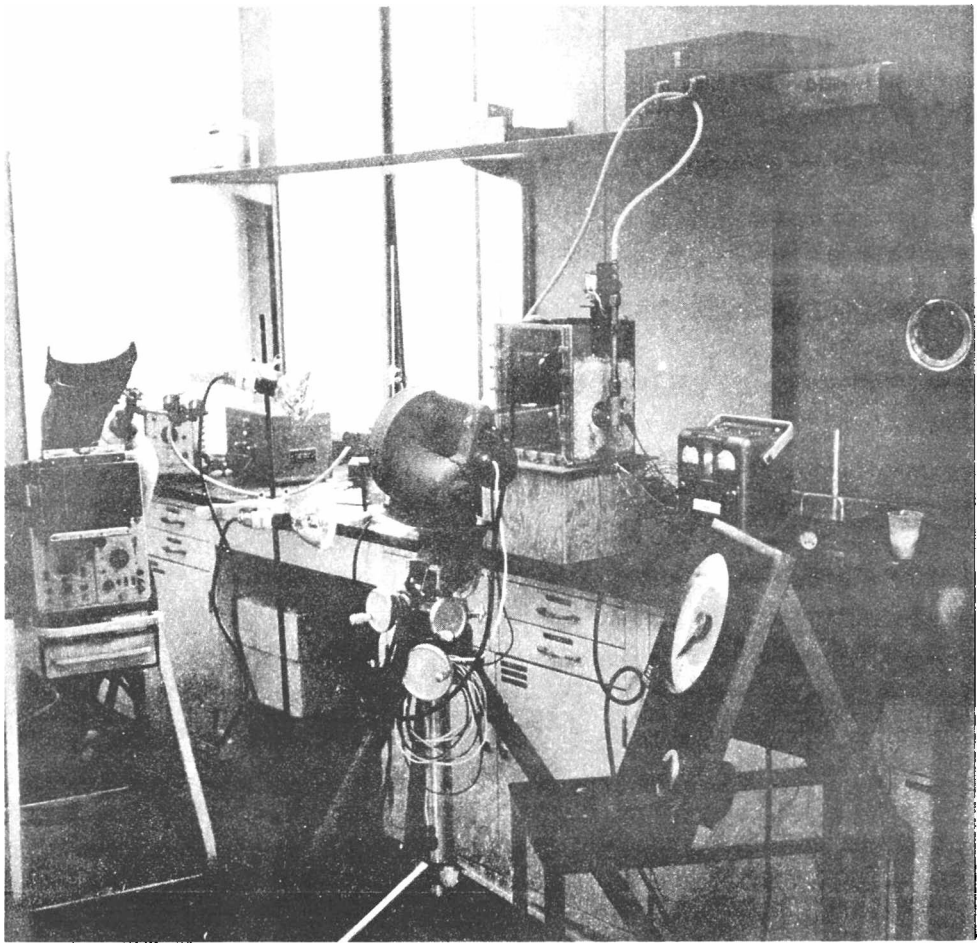

Figure 1. - Molten-metal injection apparatus

the experiment. The two side walls, the back wall, and the bottom of the tank are made of type 304 stainless steel. The front wall of the tank consists of a 0.25-inch-thick tempered plate-glass section mounted onto a flange (fig. 2). The flange has a machined groove which is filled with a bead of silicon material. The glass section is held tightly against the flange and the silicon-bead seal by a series of small aluminum clamps that are attached to the flange by screws.

Another flange with a paper gasket is mounted onto the right-side tank wall. The wall provides a machined surface on which the gate-valve assembly and the molten-metal-sample pressure-chamber assembly are mounted. This wall contains a 17-ohm resistance heater that is described in the section entitled "Sample Pressure-Chamber Assembly." Figure 3 is a photograph of the quenching-fluid tank.

MOLTEN-METAL-SAMPLE INJECTION SYSTEM

A molten-metal-sample injection system was designed to heat the sample to the desired temperature and to inject it into the tank of quenching fluid. The injection system, which is shown in figure 2 with respect to the quenching-fluid tank, consists of two basic assemblies, which are the gate-valve assembly and the pressure-chamber assembly.

Gate-valve Assembly

The gate-valve assembly (fig. 2) consists of a gate and nozzle, a mounting block, and a solenoid actuator. The gate is constructed of type 17-4 stainless steel with a Teflon insert (fig. 4). The gate-valve nozzle has 0.063-inch inside diameter with a slightly beveled

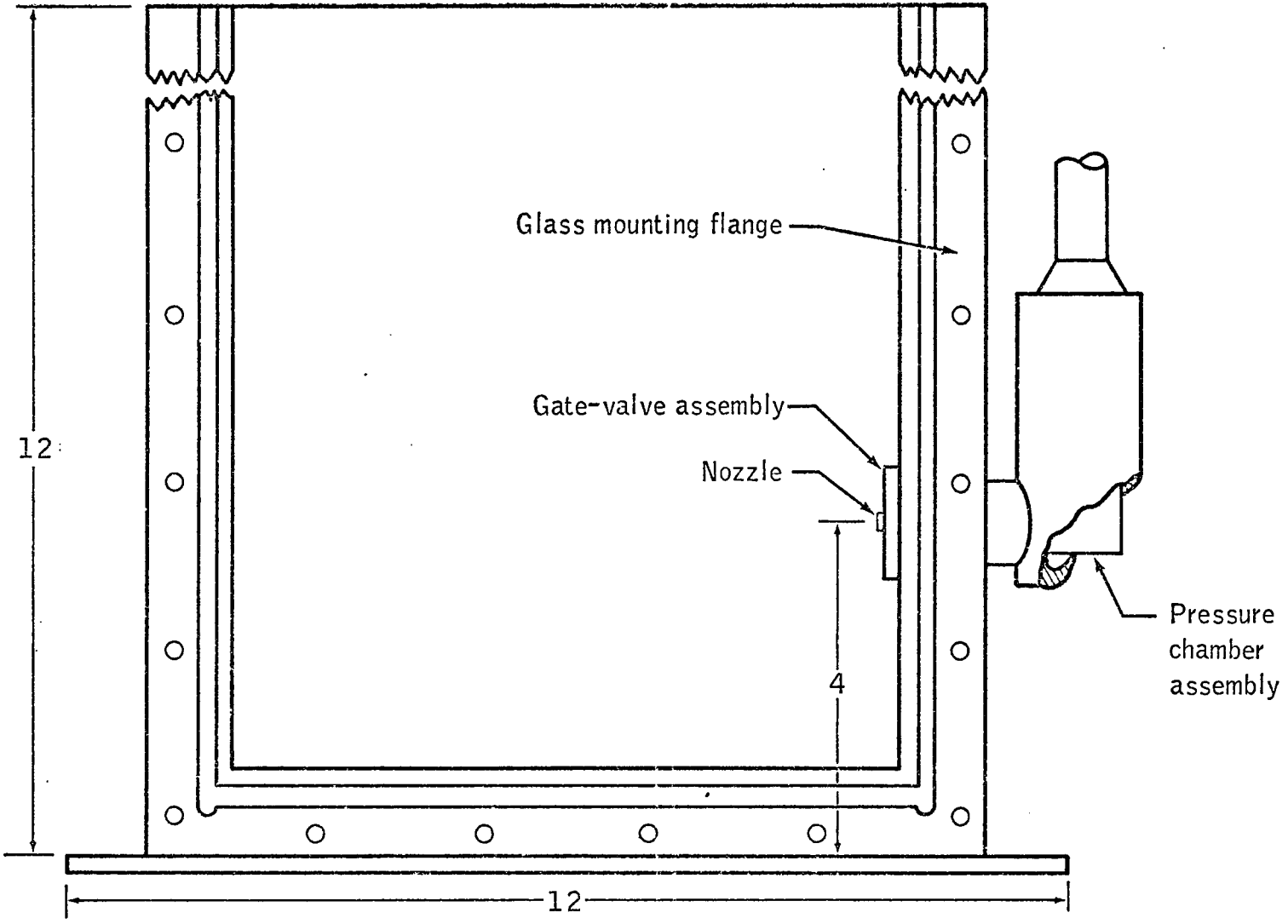

Figure 2. - Quenching-fluid tank and injection system

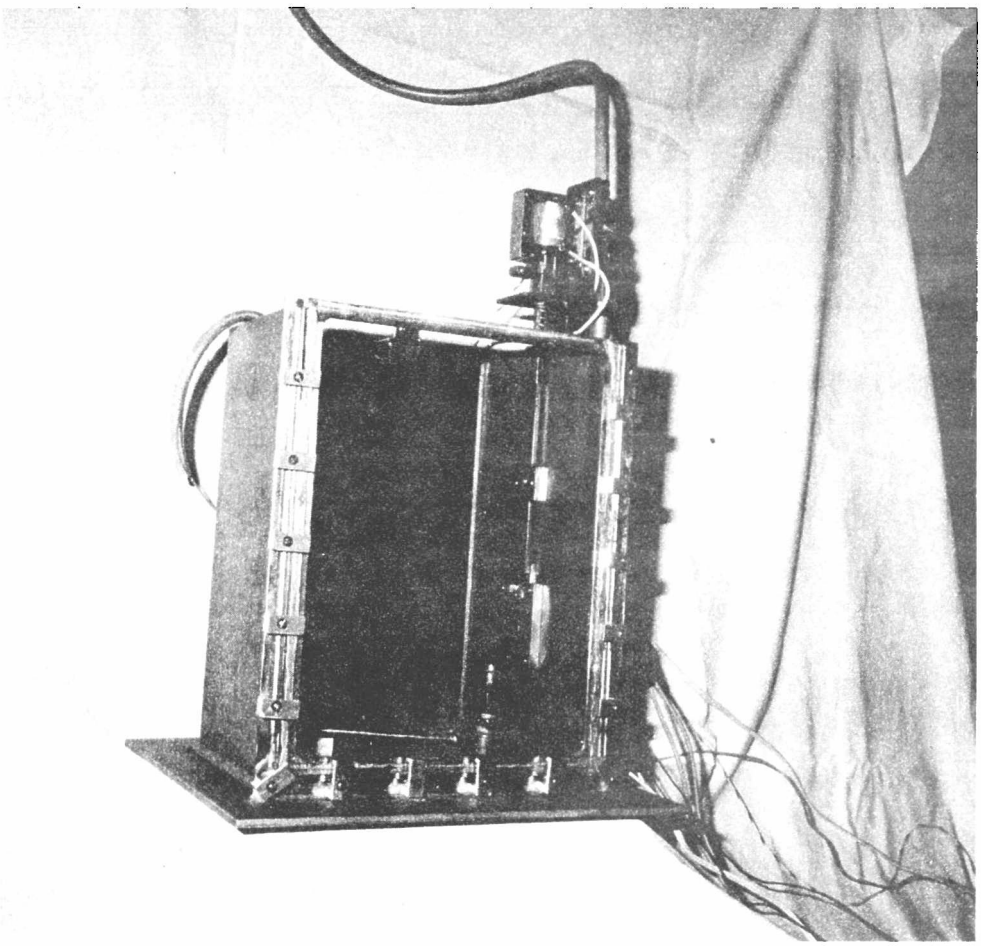

Figure 3. - Quenching-fluid tank

exit. The nozzle is drilled through a 0.15- x 0.15-x 0.25-inch extension on the stainless steel gate. A 0.040-inch-thick Teflon insert is fitted into the back of the gate to provide an easy-sliding pressure seal. The hole in the Teflon insert was reamed while the equipment was maintained at operating temperature. This was done so that the hole would have the desired dimensions when the Teflon was expanded at high temperatures.

Initially, the gate seal was obtained simply by the contact between the sample pressure-chamber tube and the stainless steel gate. After approximately 10 operations, the gate had to be reseated with a grinding compound in order to re-establish the seal. Reseating was necessary because spalling of the rubbing metals had deterioated the quality of the seal. At this point, the Teflon insert was installed to solve the problem.

The mounting block is bolted to the machined face of the quenching-fluid tank wall and holds the sliding gate-valve. The mounting block provides open and close stops for the gate. The gate-valve assembly is shown with respect to the right-side tank wall in figure 5. The rod extending out of the nozzle exit is used for calibration; its position in the figure 5 photograph indicates the trajectory of a molten-metal jet. The apparatus immediately below the nozzle exit is a pressure transducer.

A solenoid, which is mounted at the top of the quenching-fluid tank, is connected by a tensile linkage to the gate. The solenoid is spring loaded in the gate-closed position. When power is supplied to

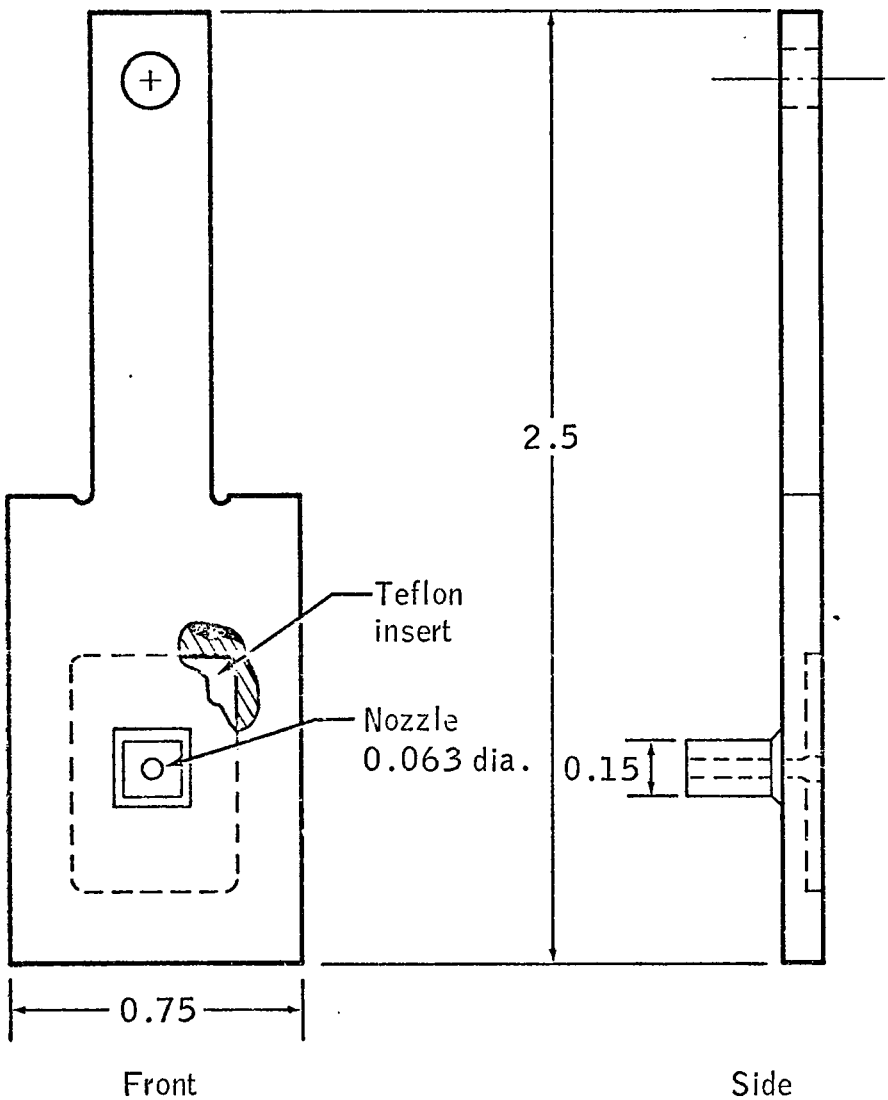

Figure 4. - Gate-valve, nozzle, and Teflon insert

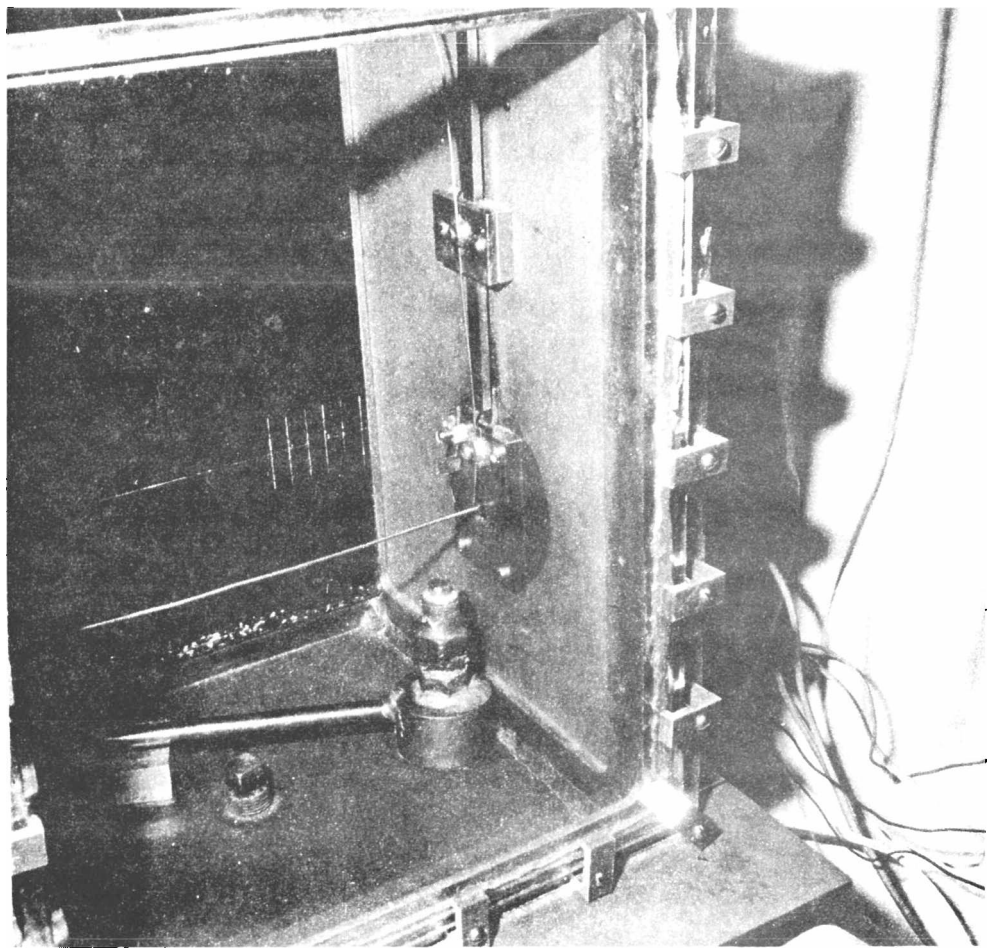

Figure 5. - Gate-valve assembly mounted on the tank sidewall

the solenoid by a push-button switch, the gate is jerked to the open position and held against the block stop. In the open position, the gate nozzle is aligned with the pressure-chamber outlet tube, and the molten-metal jet is allowed to exit into the quenching fluid. When power to the solenoid is interrupted, the gate returns to the closed position. The time required for the gate to move from the closed to the open position is less than 1 millisecond. In addition, the opening of the valve begins with a symmetrical intersection of the curved portions of two semicircles. When the valve is fully opened, a circular aperture is formed by the two semicircles. Thus, the rapidity of the gate opening and the symmetry of the opening ensure minimum distortion of the molten-metal jet.

Sample Pressure-Chamber Assembly

The molten-metal-sample pressure-chamber assembly is shown in detail in figure 6. The pressure chamber is constructed of type 304 stainless steel. A flanged tube protrudes through the quenching-fluid-tank sidewall and provides the mating surface with the gate valve for the pressure seal. The machined-on flange is mounted onto the outer surface of the quenching-fluid-tank wall, providing the primary mount for the pressure-chamber assembly. The flanged tube is welded to a larger diameter reservoir. A 0.625-inch-diameter by 9-inch-long plenum tube is attached to the top of the reservoir. The argon K-bottle pressure hose is attached to the top of the plenum tube.

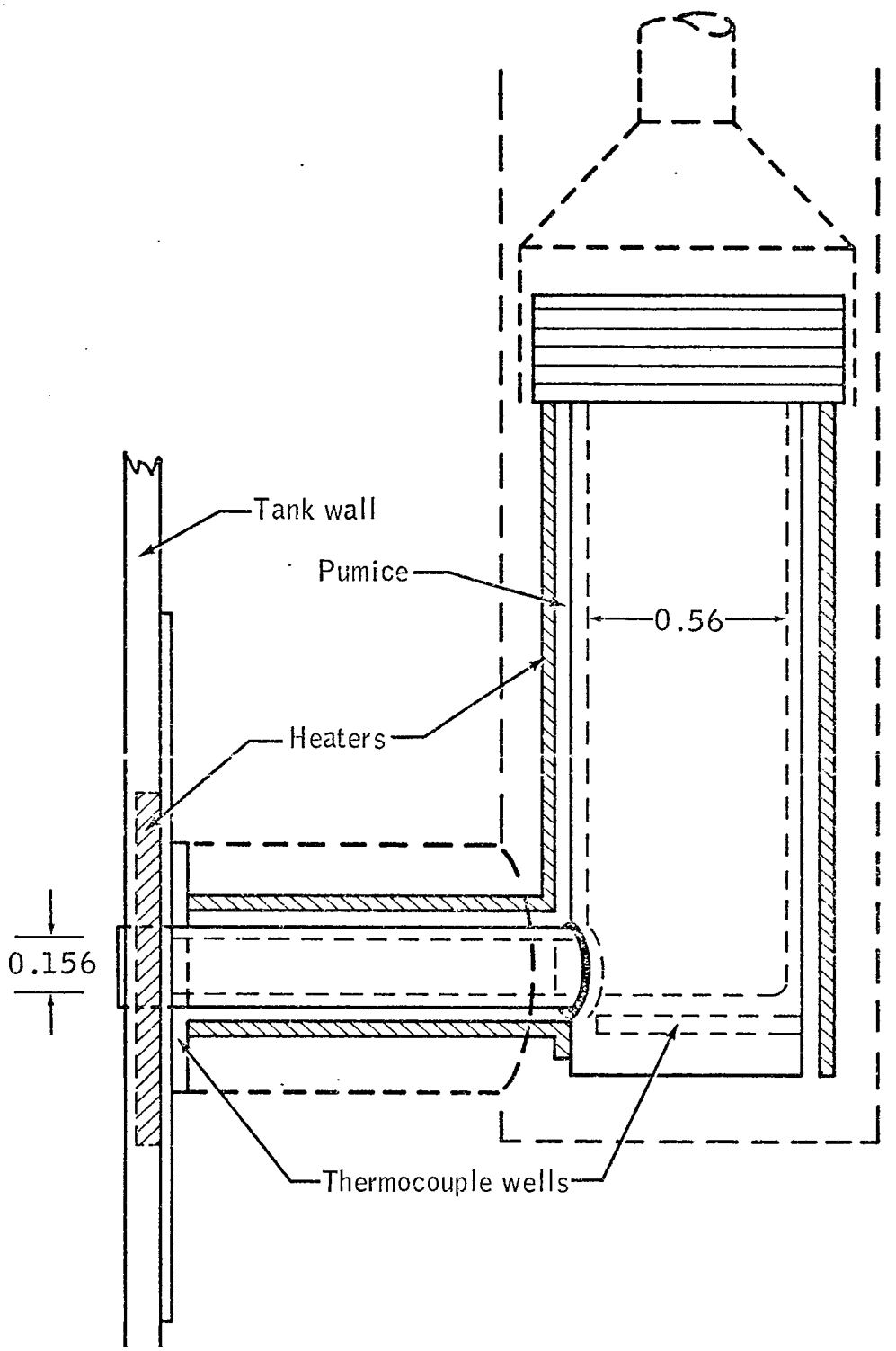

Figure 6. - Sample pressure-chamber assembly

A thin wall of pumice insulation was machined, split into two sections, and fitted around the pressure chamber (both the flanged tube and the larger reservoir). The pumice acts as an electrical insulator between the coils of the primary stainless steel pressure-chamber assembly. The primary heater is a 35-ohm resistance heater made up of Nichrome wire wrapped continuously around the flanged tube and the larger reservoir. A secondary 17-ohm resistance heater is located in a cut-out in the quenching-fluid-tank sidewall.

A stainless steel outside cover is located around the entire pressure-chamber assembly. A mineral fiber is inserted into the space between the heater coil and the outer cover to provide thermal and electrical insulation. Thermocouple wells are provided at each end of the flanged tube so that the temperature and temperature variation of the molten metal between the two ends of the flanged tube can be monitored. The molten-metal-sample pressure-chamber assembly is shown with respect to the quenching-fluid tank on which it is mounted in figure 7.

PHOTOGRAPHY AND LIGHTING

Primary Camera

The molten-metal jet was photographed with a Fastax WF 3 camera mounted on a Redlake seismic-stand tripod and operating on 120-volt AC power. At this power setting, the film framing rate peaks at 5000 frames per second after 1 second of operation. The film used in the Fastax camera was 16-millimeter Kodak TRI-X in 100-foot rolls.

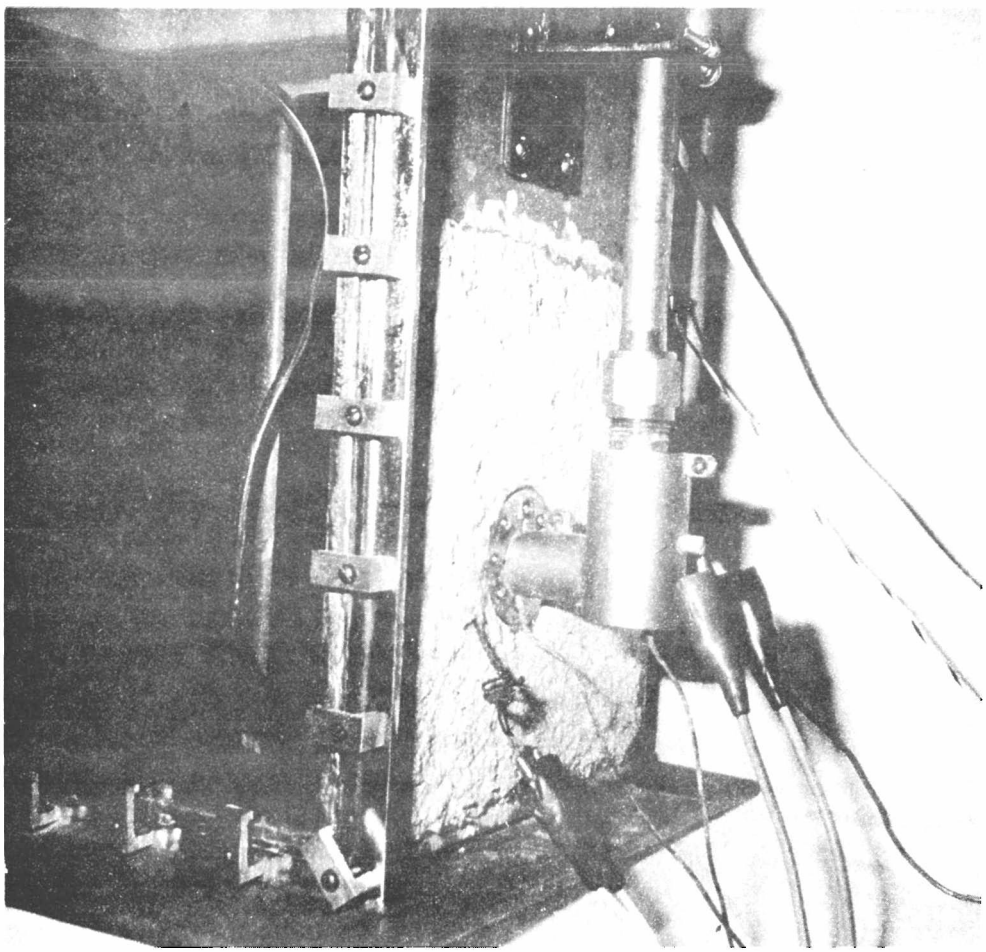

Figure 7. - Sample pressure-chamber assembly mounted on the quenching-fluid tank

The Fastax camera was started approximately 0.4 second before the gate was opened to allow the molten-metal jet to be injected into the quenching fluid. The 0.4 second period allowed the Fastax camera framing rate to reach approximately 4000 frames per second. A close-up lens was used on the Fastax camera, providing a 1.75-inch field of view at the position of the molten-metal jet.

Lighting

Two 750-watt high-intensity lights were used for lighting the molten-metal jet. Both were mounted near the Fastax camera at the front of the quenching-fluid tank approximately 10 inches from the trajectory of the molten-metal jet. One light was placed above the horizontal plane containing the molten-metal jet with the light beam striking the plane at an angle of approximately 30 degrees. The second light was placed below the horizontal plane with its beam striking the plane at an angle of approximately 15 degrees.

Still Camera

A standard Polaroid camera with a close-up lens was used to photograph the sample as it lay in the quenching-fluid tank after each firing of the jet. In addition, after each firing, the sample was removed from the quenching-fluid tank, dried, and photographed with the Polaroid camera before being stored.

4. OPERATIONAL MEASUREMENTS

SAMPLE TEMPERATURE CONTROL AND MEASUREMENT

In the sample pressure-chamber assembly, the sample was heated to the desired temperature and allowed to soak in order to achieve an even temperature distribution. The positions of the two heaters that were used to heat the sample are shown in figure 6. The heater wire that is wrapped around the main body of the pressure-chamber assembly is called the primary heater and was mainly responsible for melting the metal sample and heating the sample to the desired temperature. The heater that is located in the quenching-fluid-tank wall is called the secondary heater. The secondary heater was used to ensure an even molten-metal-sample temperature distribution by providing an extra heating capability to compensate for the heat loss through the nozzle end of the pressure-chamber assembly, which was the only part of the pressure-chamber assembly that was not covered with thermal insulation.

Metal-sample Heating

The secondary heater is a 17-ohm heater constructed from 28-gauge Nichrome wire that has been shaped into a coil with an outside diameter of approximately 0.096 inch. The coiled wire was placed in the cavity that had been machined out of the quenching-fluid-tank side wall. After insertion, the coiled wire formed a circular heating element around the part of the pressure-chamber assembly that extended through the quenching-fluid-tank wall. Current was supplied to the heater by asbestos-covered copper wires, which were run through a lead slot

between the tank wall and the flange that attached the pressure-chamber assembly to the tank. The cavity was then filled with a mineral-fiber insulation both to secure the heater coil and to provide electrical insulation.

The primary heater is a 35-ohm heater constructed from 28-gauge Nichrome wire. The wire was wrapped around a pumice-insulation layer that covers the entire pressure-chamber assembly. The pumice was machined to fit around the sample tube and the sample storage tank. The pumice-layer thickness is 1/16 inch. The primary-heater wires are wrapped around both the sample tube and the sample storage tank. The heater wires were covered with mineral-fiber insulation, and a stainless steel cover was placed around the entire pressure-chamber assembly. Currents to the heaters were supplied by two metered variacs.

Molten-metal-sample Temperature Measurements

A thermocouple was installed at each end of the sample tube to ensure that a constant temperature was maintained throughout the molten-metal sample. Both thermocouples were constructed from 28-gauge chromel-alumel thermocouple wires covered by a glass-on-asbestos insulation. The thermocouple beads were formed with a Dynatech thermocouple welder in an argon atmosphere. One thermocouple was installed under the pumice-insulation layer at the intersection of the sample tube and the flange that attached the pressure-chamber assembly to the quenching-fluid-tank wall. The second thermocouple was installed in a drilled thermocouple well 0.040 inch from the opposite end of the sample tube. The locations of the two thermocouples are shown in figure 6.

The thermocouple output voltages were fed directly into a Leeds-Northrup "Speedomax H, Type K" chromal-alumel temperature-readout device. The quenching-water temperature was measured with a standard 12-inch mercury-bulb thermometer.

SAMPLE PRESSURE CONTROL

The molten-metal sample was pressurized by argon from a standard K-bottle. The pressure reading was taken directly from the K-bottle regulator gauge. The argon was fed through a pressure line to the plenum on top of the sample storage tank. The plenum has approximately 25 times the volume of the samples used in the experiment. Preliminary investigations established that a nominal pressure of 10 psig provided a suitable jet velocity while minimizing the effects of hydrodynamic instability.

EXPLOSION PRESSURE AND FREQUENCY MEASUREMENTS

A relatively unsuccessful attempt was made to measure and record the overpressure wave propagation through the quenching fluid. The high-frequency sensitivity of the oscilloscope camera was considerably less than the high-frequency sensitivities of either the pressure transducer or the oscilloscope, and an accurate determination of the amplitude of the pressure signal was severely restricted.

Equipment

The pressure transducer that was used to measure the overpressure was a Kistler type 701. The transducer mounting was constructed from a brass fitting and a cylindrical brass block. A thin foam pad was attached to the bottom of the mounting block in order to isolate the transducer from the tank and prevent transducer detection of extraneous vibrations. The pressure-transducer assembly can be seen in figure 5.

The charge amplifier used to amplify and calibrate the pressure-transducer output signal was a Kistler S/N 425 amplifier. The charge amplifier was factory calibrated to convert the pressure-transducer output signal, which was received through a calibrated shielded cable, directly into a pressure reading according to the relation, 10 millivolts indicated after amplified for each psi detected by the pressure transducer. Other characteristics of the charge amplifier are as follows:

Parameter	Value
Range (full scale)	5,000 peb
Range capacitor	500 pfd
Output	+10 to -5 volts
Input range	1,000 psi
Sensitivity	10 mv/psi
Transducer	701 A

The charge-amplifier output signal was fed to a Tektronix Type 561 B oscilloscope, which was fitted with a Tektronix C-12 oscilloscope camera. The pressure trace that was indicated by the charge-amplifier

output was displayed on the oscilloscope screen and was photographed for each molten-metal firing run.

Pressure-Transducer Location

For the first 12 firing runs, the pressure transducer was mounted vertically against the quenching-fluid-tank side wall opposite from the injection nozzle, as shown in figure 8(a). After the completion of firing run 12, the transducer was moved to a horizontal position 11/16 inch below and 1-inch downstream from the end of the injection nozzle, as shown schematically in figure 8(b).

MOLTEN-METAL-JET VELOCITY AND SIZE MEASUREMENTS

In order to provide a frame of reference to facilitate measurement of the molten-metal-jet velocity and size, a calibrated scale was devised to provide a background for the photography. The background calibrated scale was visible in the photographs taken of each firing run. The scale itself consisted of five lines scribed onto an aluminum back plate that was painted flat black. The black back plate and scribed scale lines are clearly visible in the figure 5 photograph.

The aluminum back plate was attached to the back wall of the quenching-fluid tank. A stainless steel calibration rod 0.062 inch in diameter with scribed marks every 0.25 inch was inserted into the nozzle aperture. Thus, the calibration rod extended outward from the nozzle along the trajectory that a molten-metal jet would follow during a firing run. The quenching-fluid tank was then filled with distilled water, the quenching fluid used throughout the experiment, and the

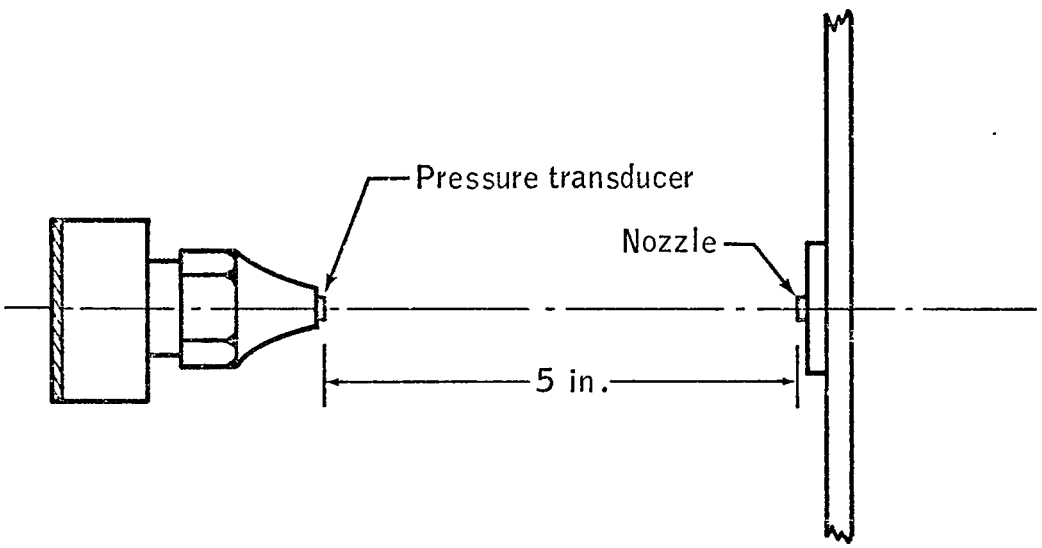

(a) Pressure-transducer location for the first 12 runs

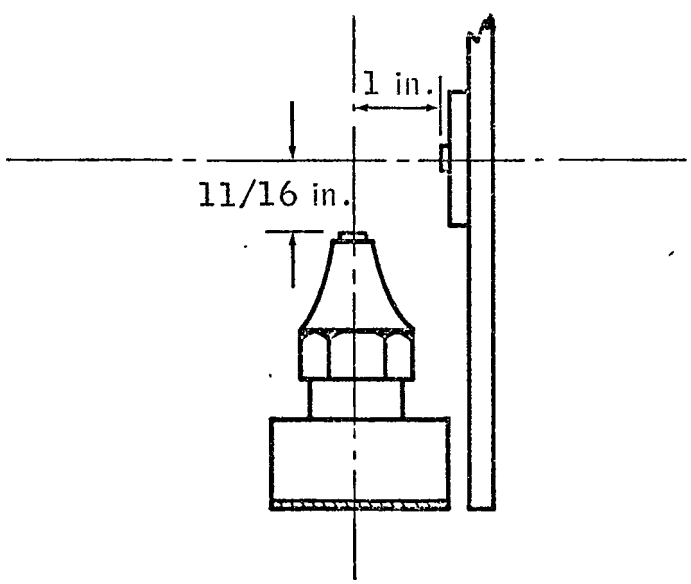

(b) Pressure-transducer location for all runs subsequent to run 12

Figure 8. - Pressure transducer location

Fastax camera was set up 14 inches from the glass front of the quenching-fluid tank, which was the desired position for photographing the jet during a firing run. The camera settings were adjusted so the camera was focused on the calibration rod. The proper positions for the reference lines on the back plate were then located by sighting through the camera lens across the reference marks on the calibration rod and onto the back plate. The reference lines were scribed onto the back plate at the points corresponding to the 0.25 inch actual distances on the calibration rod. Thus, the shiny scribed lines on the back plate provided calibrated reference lines corresponding to actual distances measured at the position of molten-metal jet. Therefore, jet velocity and size measurements could be obtained during a firing run without interfering with the jet flow patterns. Distance measurements can be made directly from the projected image of the film by using the reference lines as the proper scale. The calibrated scribed reference lines on the back plate show up on the Fastax movie film as narrow bands, since the reference lines are out of the camera plane of focus.

To obtain jet velocity data, only one other variable needs to be known, and that is the time scale. Timing marks were placed on the Fastax film by the use of a Milli-Mite Timing Light Generator, Model TLG-3, set at 1000 cycles per second. Thus, a convenient land mark or anomaly in the molten-metal jet could be selected, and the number of frames of film could be counted for the anomaly to move a prescribed distance. By knowing the framing rate of the film, as determined from the 1000-cycle-per-second timing marks, the local velocity of the jet near the anomaly could be determined.

5. OPERATIONAL PROCEDURES

The operational procedures used in conducting the experiments may be logically broken into three procedural phases, which are (1) equipment checkout, (2) verification of the desired test conditions, and (3) carrying out the experiment. A detailed checklist was used throughout each of the three phases to maintain close control of the experiment.

EQUIPMENT CHECKOUT

Each piece of equipment used in a test was checked for proper operation before the start of each test run. The molten-metal injector was carefully checked for proper operation, and cleanliness of the injector was carefully maintained to prevent sample contamination.

VERIFICATION OF TEST CONDITIONS

After each piece of equipment had been connected to the system and checked for proper operation, the desired test conditions were set up. This procedure involved the following steps.

1. The Fastax camera was carefully positioned, and the proper field-of-view and lens settings were made. The high-intensity lights were positioned, the film was loaded into the Fastax camera, and all camera settings were rechecked.

2. Argon was bled through the sample pressure chamber to remove any air, moisture, or other contaminants that might have been present in the chamber.

3. The metal sample was weighed on a standard balance scale and inserted into the pressure chamber. Argon was again bled through the pressure-chamber system and out the nozzle for several minutes to ensure contaminant removal. After the argon purge, the pressure-chamber system was closed, and a pressure of 2 psig was maintained with argon.

4. Current was then turned on to both pressure-chamber heaters to melt the sample and obtain the desired sample temperature. The current to each heater could be adjusted by a separate variable control that enabled the same temperature to be obtained and maintained at both ends of the pressure-chamber tube. This differential control of the heaters was necessary to ensure a uniform temperature throughout the molten-metal sample before the sample was injected into the quenching fluid. After the desired temperature had been reached at each end of the pressure-chamber tube and had stabilized, the system was allowed to stand for a 30-minute constant temperature soak without power-setting changes to ensure a uniform temperature throughout the molten-metal sample.

5. The molten-metal injector was tilted approximately 45° above the horizontal and shook gently to settle the molten metal against the gate and to remove any gas bubbles that may have been trapped in the molten metal. This was done at least twice before each of the constant temperature soak periods.

6. The pressure transducer was positioned, and the oscilloscope and oscilloscope camera were connected and prepared for the molten-metal injection.

7. The proper amount of quenching fluid (distilled water) was measured into a container, and the temperature of the quenching fluid was measured. Any adjustments to the quenching fluid temperature were made by adding chilled or heated distilled water.

8. The argon pressure was increased to 10 psig.

9. A final check was made before the test was run and all test conditions were recorded.

TEST RUN

The carrying out of an actual test run took only a matter of seconds, after the desired test conditions had been verified. The procedural steps involved in a test run are as follows.

1. A final check was made of all equipment and test conditions.

2. The high-intensity lights were turned on low.

3. The distilled water that had been previously measured out to give the desired level in the quenching-fluid tank was poured into the quenching-fluid tank.

4. The oscilloscope used to display the pressure-transducer output was reset on external trigger.

5. The distilled water was allowed to settle for 3 or 4 seconds. A longer wait for the water to settle would have been desirable; however, a longer wait period would have allowed a cooling of the molten-metal injection nozzle and an upsetting of the uniform temperature of the molten-metal sample itself. Thus, the 3- to 4-second wait period was chosen as the best time for achieving the best overall results.

6. The Fastax camera was started manually and allowed approximately 0.4 second to obtain a framing rate of approximately 4000 frames per second. Then, current was supplied to the injection-gate solenoid, and the gate valve was opened.

7. The equipment was shut off.

8. The metal-sample residue was photographed in the tank after the distilled water had been removed. The residue was again photographed after it had been removed from the tank, and then it was stored.

6. EXPERIMENTAL RESULTS

A total of more than 200 runs were made with the experimental equipment. These runs consisted of development, preliminary, and operational runs. Mercury was used for most of the early tests for check-out of the equipment, development of the test procedures, and assessment of the hydrodynamic stability of the jet. Fifty-four operational firing runs were conducted, and data were recorded for each run. Of the 54 operational runs, 48 provided useful data. The remaining six runs were about equally divided between bad photography and flow stoppage due to solidification of the sample in the nozzle.

MERCURY RESULTS

Three operational firing runs were made using mercury as the molten metal. The mercury which had a temperature of 550°F for all three runs, was injected at pressure of 10 psig. All three runs were similar in appearance with a number of vapor explosions occuring during each run. The first two runs were almost identical and the third run displayed somewhat less explosive action. Several items of particular interest were noted.

1. The mercury jet did explode.

2. The maximum diameter of the exploded jet was consistently observed to be approximately 0.2 inch.

3. The distance from the end of the nozzle to the center of the explosions was consistently observed to be approximately 0.1 inch.

4. Several of the explosions were violent enough to halt the mercury flow from the injection nozzle.

The average velocity of the mercury jet during the first two firing runs was 93 in/sec, and the average velocity for the third run was 82 in/sec. This 11-inch-per-second velocity difference probably accounts for the lower explosive action observed during the third firing run as compared with the explosion action observed during the first two firing runs.

Most of the mercury particles (at least 95 percent) that had been ejected from the jet by the explosions were concentrated in a band approximately 0.2 inch in diameter. This particle distribution seemed to remain stable for several frames of the Fastax camera film, before the mercury particles began to disperse from the band as they moved downstream. The size of the dispersed mercury particles was 0.002-inch diameter or less for most of the particles (again, for at least 95 percent).

A number of explosions that were observed during each of the three firing runs were violent enough that the mercury-jet flow from the nozzle was completely stopped. Several explosions were of such magnitude that backflow into the nozzle was observed. That is, mercury from the jet was propelled back into the injection nozzle. This indicated that the explosion overpressure was greater than the jet injection pressure, which was 10 psig.

The mercury seemed to explode with small sharp blasts that left the major portion of the material within a radius of approximately 0.10 inch from the center of the jet. Smaller particles were blown out to radii of greater than 0.10 inch, but usually less than 0.20 inch.

Several of the explosions were preceded by the appearance of a shadow on the jet near the point where the explosion subsequently occurred. The shadow on the jet appeared to be an irregularity in the vapor boundary layer between the jet and the quenching fluid. However, this explanation is speculative, and was neither supported nor refuted by any of the experimental data collected.

Several of the observed explosions were preceded by a noticeable bulge in the jet at the point where the explosion subsequently occurred. The bulge was usually visible for two or three frames (approximately 0.75 millisecond) before the actual explosion, and the duration of the explosion was usually one frame or less than 0.25 millisecond.

The mercury jet exhibited normal stability immediately after it had left the injection nozzle. However, approximately 0.5 inch downstream from the end of the nozzle the jet began to experience Helmholtz instability; and at all distances greater than 0.5 inch from the end of the nozzle, Helmholtz instability was evident.

A smoke-like layer with a slightly bluish tint emanated from the mercury jet and spread outward in all directions from the jet. The layer around the jet had a radius of approximately 0.05 inch at a distance of 1.0 inch from the end of the nozzle. A chemical analysis of water used during a firing run revealed the presence of only pure mercury in the water. The concentration of mercury in the water was found to be 190 parts per billion.

ASARCOLO 158 RESULTS

Twelve operational molten-metal-jet firings were made using Asarcolo 158. The firing series was begun with the molten Asarcolo 158 at 210°F, and ranged up to 600°F.

During the operational firing series, the following items of interest were noted.

1. Explosions were observed when the molten Asarcolo 158 was injected at a temperature of 210°F.

2. The distance that explosions occurred from the nozzle and the size of the explosions were functions of the molten-metal temperature.

3. When the jet was fired with the molten-metal temperature at 300°F or below, the occurrence of the explosions, the distances of the explosions from the nozzle, and the sizes of the particles that resulted from the explosions were all somewhat erratic.

4. The sizes of the particles ejected from singular explosions were predominately from 0.002 to 0.005 inch in diameter and smaller.

5. When the jet was fired with the molten-metal temperature at 400°F, the resulting explosions were fairly consistent and predictable. The explosions occurred approximately 0.08 inch downstream from the nozzle, approximately 0.25 to 0.50 millisecond after the material involved in the explosion had left the nozzle. The diameters of the explosions were 0.15 to 0.20 inch.

6. When the jet was fired with the molten-metal temperature at 400°F, a noticeable water-vapor film was present.

7. With the molten-metal temperature at 400°F, the resulting explosions were sometimes violent enough to cause flow stoppage. These more violent explosions had a diameter of approximately 0.25 inch.

8. With a molten-metal temperature of 400°F, some "popcorn" expansion (resulting in a high porosity residue core) of the molten-metal jet was observed approximately 0.50 inch downstream from the nozzle.

9. With the molten-metal temperature at 400°F, a cycle was observed of jet protrusion approximately 0.1 inch out of the nozzle, followed by an explosion that propagated upstream to the nozzle exit. The jet then re-emerged and the cycle repeated.

10. With the molten-metal temperature at 500°F, the resulting explosions were sometimes severe enough to cause a reverse flow at the injection nozzle.

11. With the molten-metal temperature at 500°F, the explosions occurred just outside the nozzle (at approximately 0.04 inch from the nozzle) and were almost continuous with some cycling observed at a high frequency (approximately 1-millisecond period).

12. With the molten-metal temperature at 500°F, some explosions were observed farther downstream from the nozzle. These downstream explosions occurred as the jet passed through large concentrations of vapor near the nozzle.

13. With the molten-metal temperature at 600°F, almost no continuous jet was visible. The explosions occurred 0.02 to 0.04 inch downstream from the nozzle. Most of the scatter that resulted from the explosions was obscured by large concentrations of vapor.

The experimental evidence indicated that the distance of the explosions from the end of the nozzle and the size of the explosions were definitely functions of the molten-metal temperature. For each molten-metal temperature, the distances from the nozzle of several explosions were averaged, and the results are plotted in figure 9. Use of average values in figure 9 gives an accurate representation of the trends that were observed.

The data points representing the first set of data (at 210°F) are somewhat off from the points predicted by the extrapolated curves. That is, the average diameter of the explosions of a jet of molten Asarcolo 158 with a temperature of 210°F is less, and the average distance from the end of the nozzle that the explosions take place is greater than the predictions of the respective curves. This phenomon indicates that for molten Asarcolo 158 with a temperature of 210°F, a minimum explosion threshold strength exists, below which an explosion will not occur. The extrapolated curve predicts an explosion with a strength below the minimum for the given set of conditions (Asarcolo 158 at a temperature of 210°F), and thus, the predicted explosion did not occur. Likewise, for the given set of conditions, the distance that an explosion occurs from the end of the nozzle has a maximum limit, beyond which explosions will not occur. The extrapolated curve predicts the occurrence of an explosion beyond the threshold, and thus, the explosion did not occur.

A similar trend was evident in the dimensions of the sample residues. The lowest molten-metal temperature resulted in the largest residue-particle size. The residue-particle size decreased as the

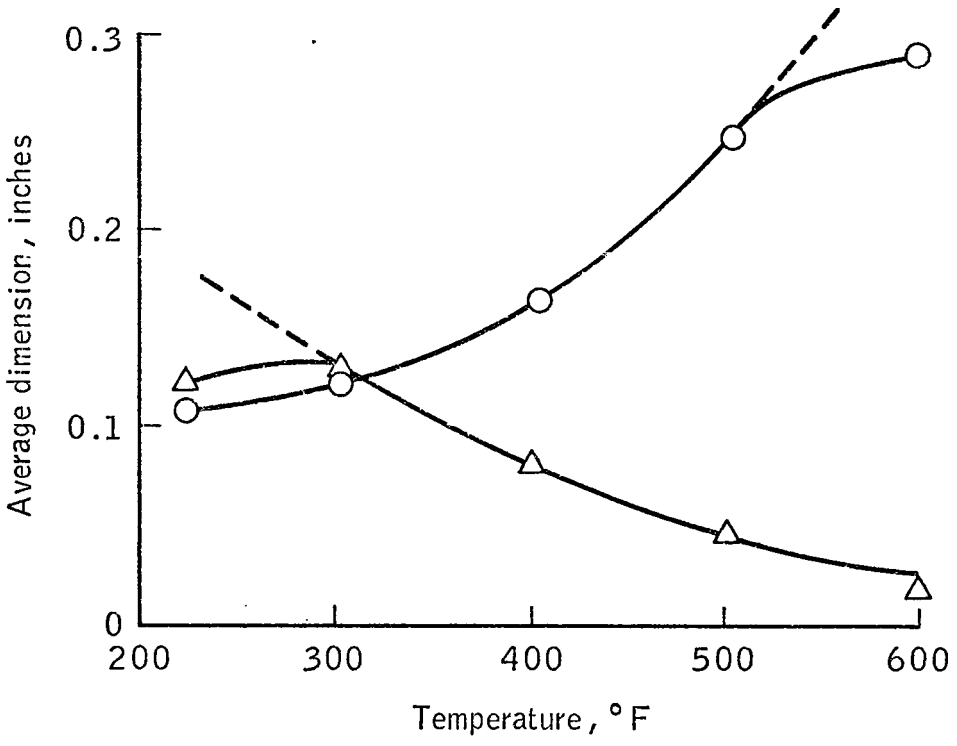

Figure 9. - Asarcolo 158 explosion trends

temperature of the molten metal that was injected was increased, which is what would be expected knowing that the violence of the explosions increases with increasing molten-metal temperature.

The Asarcolo 158 jets with a temperature of 300°F and below were generally stable for the first 0.75 to 1.00 inch after leaving the nozzle. After the first 0.75 to 1.00 inch, the jet seemed to acquired Helmholtz instabilities. No solidification of the jet was evident from the Fastax-camera photographs which record data to a point approximately 1.5 inches downstream from the end of the nozzle. Very little vapor was observed during any of the firings of Asarcolo 158 with a temperature of 300°F or less.

With the molten Asarcolo 158 at 400°F, the explosions were considerably more violent than they had been when the metal temperature was 300°F. A water vapor film was observed for the first time during the firings with the Asarcolo 158 at 400°F. The vapor film was irregular in thickness, but appeared to be 0.015 to 0.020 inch thick. The explosion phenomenon had a definite cyclic nature. The molten Asarcolo 158 jet would leave the nozzle and travel approximately 0.1 inch (or two jet diameters) without the loss of the jet structure. Then, an explosion would take place just behind the tip of the jet, the explosion would propagate along the jet back toward the nozzle and would stop at the nozzle. At this point, the cycle would begin again with a stable jet exiting the nozzle. The period of a cycle was approximately 4 milliseconds.

With the molten Asarcolo 158 at 400°F, the explosions occasionally were violent enough to cause stoppage of the molten-metal flow from the nozzle. The explosions were located approximately 0.08 inch from the nozzle exit, and the explosions caused the jet to expand at the point of the initial explosion to a diameter of slightly less than 0.20 inch. The more violent explosions that resulted in a stoppage of molten-metal flow at the nozzle would expand to a diameter of approximately 0.25 inch. The duration of the stoppages was from 3 to 5 milliseconds. After a flow stoppage, the jet would reappear for a period of 5 to 8 milliseconds as more of a spray, before settling back to a stable jet.

Another interesting phenomenon was observed during the firings of molten Asarcolo 158 at a temperature of 400°F. Starting at approximately half way through a run, a conical vapor shield would form around the molten-metal jet and the nozzle face. The vapor shield was present periodically during the second half of a run and can be seen in figure 10. When the vapor shield was present, the centers of the explosions, which had initially been located approximately 0.1 inch from the end of the nozzle, were moved downstream to a point approximately 0.3 inch from the end of the nozzle.

With the molten Asarcolo 158 a temperature of 500°F, almost no stable jet was observed beyond at point approximately 0.25 inch downstream from the end of the nozzle. The explosions occurred almost continuously. They were located 0.04 to 0.05 inch downstream from the nozzle, except when the molten-metal jet and the nozzle face were surrounded by a vapor shield. More vapor was generally present than

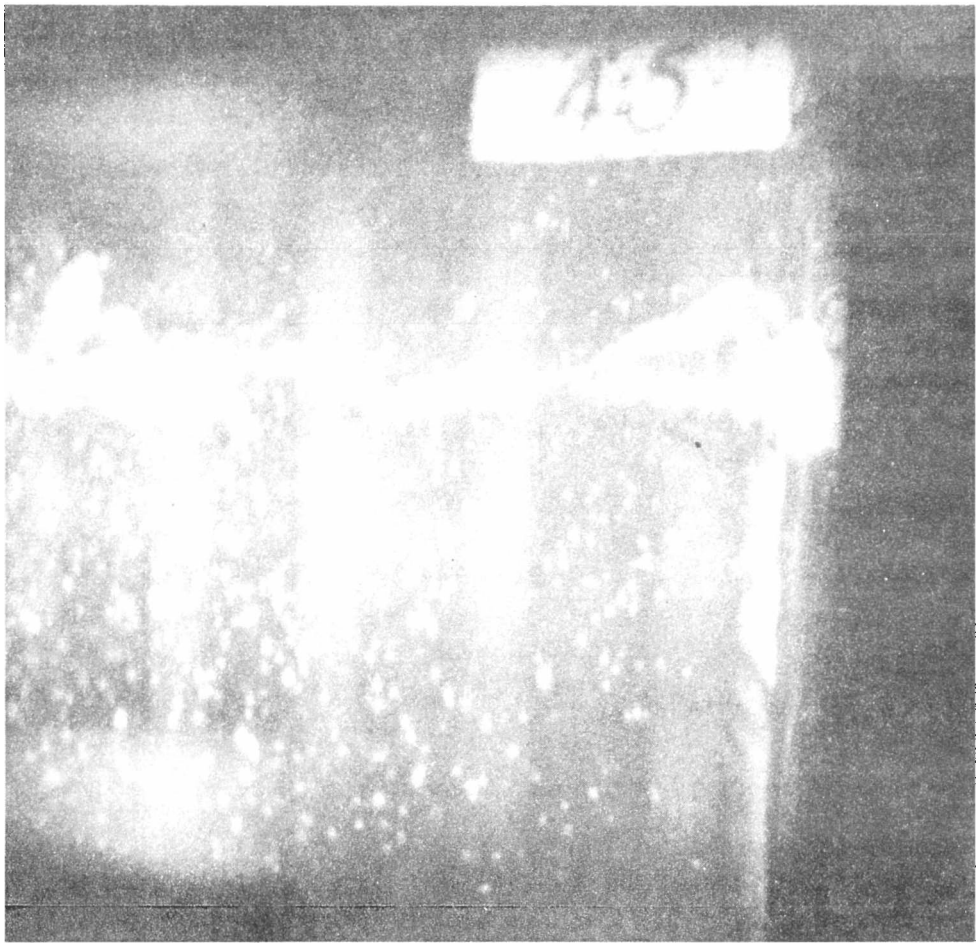

Figure 10. - Conical vapor shield

had been observed during the firings at 400°F. The vapor shield around the jet and the face of the nozzle was less stable than it had been during the firings at 400°F. The vapor shield was often broken by the agitation that resulted from the more violent explosions. Occasionally the molten-metal jet would begin pulsing through the conical vapor shield and would continue pulsing for eight or ten cycles. A cycle was characterized by the jet traveling stably through the vapor shield to a point approximately 0.25 inch downstream from the exit of the nozzle. At this point, an explosion would occur, as the jet attempted to pass through the small end of the conical vapor shield. The result of the explosion would be the collapse of the vapor shield, which would be followed by the emerging from the nozzle of a new segment of the jet, the formation of a new vapor shield, and thus, the start of a new cycle.

When the conical shield was not present or when it did not predominate the phenomenon (approximately one-half the duration time of a run), the same type of cycling was observed as has been desdribed for the molten Asarcolo 158 firings when the molten-metal temperature was 400°F. The only difference was that with the molten-metal temperature at 500°F, the explosion frequency was higher, and thus, the distance from the end of the nozzle that the explosion occurred was shorter. The cycles were characterized by the protrusion of a stable molten-metal jet to a point approximately 0.05 inch from the end of the nozzle, the occurrence of an explosion near the downstream end of the jet, and the propagation of the explosion back to the nozzle exit. With the emergence of a new segment of the jet from the nozzle, a new cycle would begin. The period of a cycle was 0.8 to 1 millisecond.

With the molten Asarcolo 158 at 500°F, almost every explosion stopped, or at least slowed, the jet flow momentarily. Many of the explosions even caused a back flow in the injection nozzle. With the molten metal at 500°F, the jet velocity could not be measured because of the almost continuous back flow and stoppage and because of the almost instantaneous jet disintegration that resulted from the violent explosions. These phenomena seemed to indicate that with the molten-metal temperature at 500°F, the threshold had been reached where the pressures generated by the explosions were on the order of 10 psig (the pressure at which the molten metal was being injected). As was the case at 400°F, the jet was surrounded by water vapor with a vapor-film thickness of from 0.015- to 0.020-inch. The centers of the explosions generally were located from 0.04 to 0.05 inch from the end of the nozzle, except when a predominating vapor shield was present, which enabled the jet to travel approximately 0.25 inch downstream before the explosion occurred.

The propagation of the explosions along the jet was not a smooth phenomenon. The jet simply appeared to experience a sudden increase in diameter, followed by the disintegration of the molten metal into small particles, usually with a diameter of 0.005 inch or less. As mentioned previously, the occurrence of the explosions was a cyclic phenomenon with a period of 0.8- to 1.0-millisecond.

With the molten Asarcolo 158 at a temperature of 600°F, the jet was almost totally obscured by large concentrations of vapor. The explosions occurred from 0.02 to 0.04 inch from the end of the nozzle,

closer than had been observed during the lower temperature firings. The particles that resulted from the very violent explosions were also more widely scattered than had been observed after firings under lower temperature conditions. The explosion caused the main body of the jet to extend to a diameter of 0.25 to 0.30 inch, but the great extent of the final particle scatter is not indicated by this explosion diameter. Little evidence was observed of the cyclic explosion characteristics that had been evident during the molten-metal firings under lower temperature conditions.

Throughout the firing runs of the molten Asarcolo 158 (at all temperatures), pressure-wave data were recorded on film by photographing the oscilloscope response to the pressure-transducer output. The pressure-pulse frequencies were difficult to determine because of lack of photographic resolution and because of the distortions caused by pressure-wave reflections. However, approximate frequencies were obtained, and these are shown in figure 11. The pressure-pulse frequency was found to increase greatly as the molten-metal temperature was increased. Enough uncertainty exists in the pressure-wave data plotted in figure 11 that the curve cannot be considered to be a true representation of the magnitude of the frequency counts. However, the general trend indicated by the figure 11 plot is accurate.

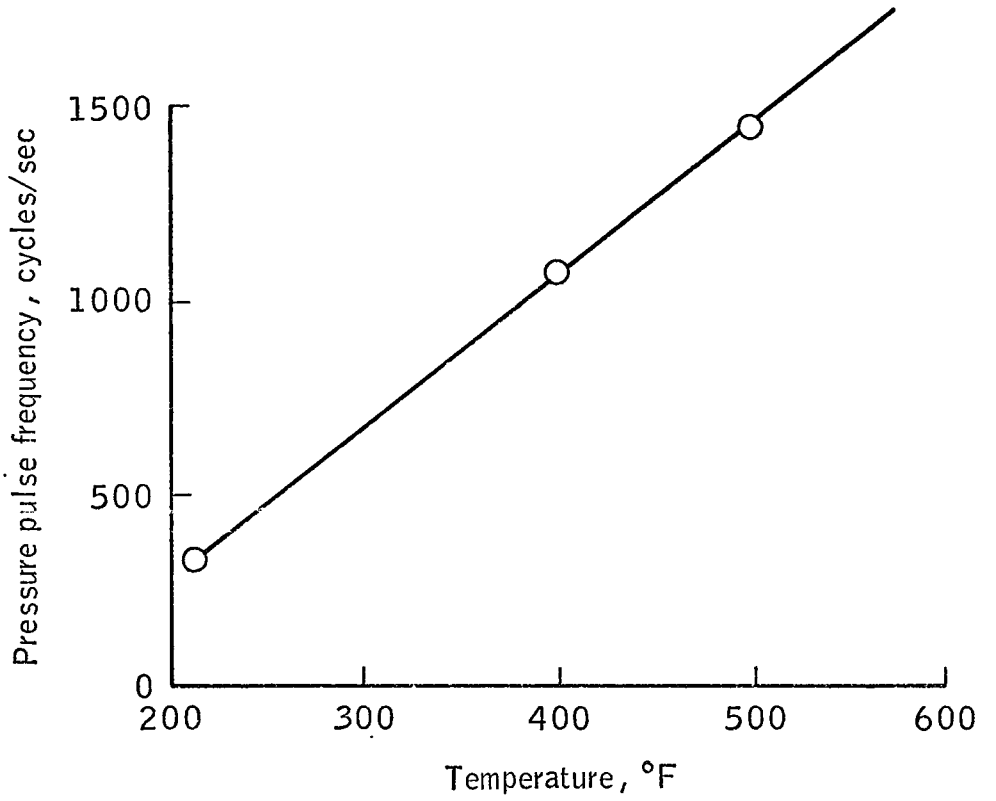

Figure 11. - Pressure-pulse frequency as a function of sample temperature for Asarcolo 158

LEAD-TIN ALLOY RESULTS

With a lead-tin alloy (50% Pb - 50% Sn by weight) used as the molten metal sample, a total of 15 operational firing runs was made. The lowest alloy sample temperature used during any operational firing run was 500°F. The reason for this was that during preoperational test firing runs, essentially no explosive action was observed for sample temperatures less than 500°F. Also, at sample temperatures below 500°F the injection nozzle often became clogged because of molten-metal solidification in the nozzle. The injection pressure used throughout the operational firing runs was 10 psig, which produced an average jet velocity of 95 in/sec. For the operational series the sample temperature was increased in increments of 50°F from 500°F to 650°F.

For the lead-tin alloy, 500°F appeared to be the approximate threshold temperature at which explosive action first occurred. At 500°F, the jets solidified, for the most part, with evidence of only intermittant explosive action. The action, when it did occur, was usually a smooth swelling of the jet, with solidification occurring before the jet could be torn apart (popcorn expansion). The action was something less than the violent explosive action that would fragment a molten-metal jet. The residue of a firing run was, then, a single core of lead-tin alloy relatively smooth with occasional high porosity swelled segments that had resulted from the low explosive action during the firing run. Some smooth voids were also evident in the core of the alloy strand. Only small amounts of alloy residue that had been fragmented or separated from the main strand of the solidified jet was recovered from the tank.

The average jet velocity during the firing runs at a temperature of 500°F was 98 in/sec, with a jet velocity range of 75 to 115 in/sec. In some cases, a slight hangup or stoppage occurred as the nozzle gate was first opened. This short-duration stoppage was accompanied by the formation of vapor in front of the nozzle. The short pause was terminated by the emergence of the molten-alloy jet at a higher velocity than observed in the cases where no initial stoppage occurred. The jet would quickly decelerate to a velocity of approximately 100 in/sec. This deceleration occurred within 1 inch of the nozzle.

The average distance of the popping action from the end of the nozzle was 0.15 inch, with the distance ranging from 0.12 to 0.18 inch. The average jet diameter at the points where swelling had occurred was 0.14 or 0.15 inch and the rest having diameters of 0.08 to 0.20 inch.

Solidification of the jet appeared to be almost instantaneous after a pop and the resulting swelling had occurred. However, for a jet segment that did not experience any pops and swelling, the solidification distance was approximately 0.63 inch downstream from the end of the nozzle. The solidification distance was stable throughout all of the 500°F firing runs, and the only variation in the distance appeared to be the result of variation in the jet velocity.

With the molten-alloy temperature at 550°F, the explosive action was still not fully developed. Long segments of the solidified jet core were characterized by the popcorn type of expansion that resulted from the firing runs with a sample temperature of 500°F; however, some segments of the solidified jet were relatively smooth, which indicated

that little or no explosive action had occurred within these segments. A thin vapor layer could be seen around the jet, but the large conical vapor shield appeared only once, and it collapsed after only a brief period. A few marginal flow stoppages were observed, but the explosions (or pops) were generally too weak to stop the jet flow.

The average velocity of the jet for the segments of the jet that experienced no explosive action was determined to be 94 in/sec, with a velocity range of 88 to 96 in/sec. For the segments of the jet that had experienced explosive action resulting in popcorn expansion, the jet velocity was reduced to a range of 60 to 70 in/sec. This velocity reduction resulted in additional stacking of the molten alloy, which extentuated the rough popcorn appearance of those jet segments.

The average distance of the explosive action downstream from the end of the injection nozzle was 0.10 inch, with most of the activity occurring within a range of 0.08 to 0.11 inch. However, a few instances of explosive action were observed approximately 0.20 inch from the end of the nozzle. The average diameter of the jet segments that had experience explosive expansion was 0.15 inch, with a diameter range of 0.08 to 0.20 inch. More than half of the diameter measurements were 0.15 inch. Examination of the Fastax film after the firing runs and examination of the solidifed jet cores recovered after the firing runs revealed that in some instances as much as 0.5 inch of the jet had experienced uninterrupted popcorn expansion as the result of a continuous explosive action. For the cases where the explosions (or pops) were discrete and were not a part of some continuous explosive action,

the average diameter of the jet segment that had been expanded by the explosion was determined to be 0.14 inch.

The explosions were sometimes preceded by the formation of a bulge that showed stable expansion for one or two film frames before popping on open to the diameter at which it would finally solidify. For a discrete or isolated explosion, the complete explosion process (from the initial detection of a bulge through the expansion of the jet to its maximum diameter) required an average of 0.8 millisecond. The explosion process itself (from the initial pop or breaking of the jet through the expansion of the jet to its maximum diameter) required approximately 0.2 millisecond.

Several cases of explosion propagation were observed in which an explosion would occur at some point on the jet and then would propogate in either direction along the jet. In only one case could the propagation rate be estimated, and the rate was found to be 550 in/sec.

With the molten lead-tin-alloy temperature at 600°F, the explosive potential was fully developed, and the explosive action was essentially continuous. Completely continuous explosive action was not achieved, however, because of the periodic interference from the thick vapor film that was present. A conical vapor shield, which was described previously in the section entitled "Asarcolo 158 Results" and shown in figure 10, appeared frequently during flow stoppages and restarts. After re-establishment of jet flow subsequent to a flow stoppage, the vapor shield would remain intact approximately 4 milliseconds, with shield collapse occurring as the jet penetrated the small end of the conical

shield. The shield collapse was presumably caused by the circulation of the cooler water along the jet, as is described in the section entitled "Boundary-Layer Location." The molten-alloy jet would explode immediately after it had penetrated the small end of the conical shield.

With the molten-alloy temperature at 600°F, the magnitudes of the explosions were usually large enough to halt the jet flow. Some long-duration flow stoppages (up to 100 milliseconds), which were accompanied by backflow, were observed; and numerous short-duration flow stoppages (approximately 0.25 millisecond) without backflow were observed.

The average diameter of the explosion-expanded segments of the jets was 0.19 inch, with a diameter range of 0.13 to 0.30 inch. The most commonly observed diameter, however, was approximately 0.20 inch. The lengths of the jet segments that were expanded by discrete or isolated explosions ranged from 0.20 to 0.25 inch. The downstream distances from the end of the nozzle at which the explosions occurred ranged from zero to 0.05 inch. Most of the discrete or isolated explosions occurred approximately 0.05 inch downstream from the exit of the nozzle. The average velocity of the short, relatively undisturbed segments of the jets was determined to be 93 in/sec, with a velocity range of 77 to 110 in/sec.

Occasionally, the jet flow would be accompanied by a pulsation (expansion and collapse) of the thick vapor shield that surrounded the jet. One series of pulsations was observed which included 7 complete expansion and collapse cycles. For this particular series, the average pulsation frequency was determined to be 1450 cycles per second.

During the firing runs with the molten-alloy temperature at 600°F the explosions would propagate downstream along the short, relatively undisturbed segments of the jet. The propagation rate was difficult to determine because the jets were usually too ragged or broken for accurate estimates to be made. Estimates were made for four fairly smooth segments of the jet, and the propagation rates were determined to be 400, 275, 240, and 330 in/sec, respectively, with an average propagation rate of 311 in/sec.

With the molten-alloy temperature at 650°F, numerous explosions produced overpressures that were considerably greater than the molten-metal injection pressure of 10 psig. In one case, 10.7 grams of the 16-gram sample were recovered from a brass fitting that was located above the pressure plenum tube. The brass fitting was located 12 inches above the horizontal plane that contained the molten-metal-jet trajectory, and the recovered sample residue was plastered tightly in a crevice of the fitting, which indicated that the residue had struck the fitting with a relatively high velocity.

With the alloy temperature at 650°F the molten-alloy-jet velocity was highly erratic, with many stoppages occurring during each firing run. The diameter of the exploded segments of the jet ranged from 0.20 to 0.35 inch, with an average exploded-jet diameter of 0.26 inch. The downstream distance of the explosive action from the injection nozzle varied from almost zero to approximately 0.03 inch. Some cases of explosion propagation along the molten-alloy jet were observed, but the jet was so turbulent that no useful propagation-rate data could be obtained.

Subsequent to some of the larger explosions, sample back flow would occur, and water and water vapor were forced into the nozzle by the overpressure. Once inside the pressure chamber the water and water vapor apparently mixed with the molten-alloy; and when the explosion overpressure had been overcome by the 10 psig molten-metal injection pressure, the jet flow would resume with the injection of the mixture into the quenching fluid. The large amount of water vapor injected into the quenching fluid after a backflow had occurred plus the large amount of water vapor that always formed around the jet as a result of the high jet temperature acted to effectively obscure the jet from view in most cases.

The low-temperature threshold of explosive action for the lead-tin alloy injected at a pressure of 10 psig was 500°F. With an initial temperature of 500°F, the molten-alloy jet solidifed after showing very little explosive action, except for a few intermittent, isolated explosions. As the initial temperature of the molten alloy jet was increased, both the frequency and violence of the explosions also increased. For molten-alloy injection at 650°F, essentially all of the jet exploded into a high-porosity core with a length of 0.5 inch or less.

The size of the sample residue that is recovered after a firing run is a good indication of the magnitude of the explosion that shaped the residue. A residue diameter of 0.20 inch indicates that the overpressure magnitudes were on the order of the magnitudes necessary to cause jet-flow stoppages. A residue diameter of 0.25 inch indicates that the overpressure magnitudes were large enough, under normal circumstances, to cause a reverse flow of the jet, which also implied the

flow of water and water vapor in an upstream direction through the injection nozzle and into the pressure chamber.

The average sample residue diameter after an explosion is plotted as a function of initial molten-alloy temperature in figure 12. Each data point on each of the figure 12 curves represents the average measured size of the parameter for that particular temperature.

The downstream distance of the center of the explosive action from the end of the injection nozzle was consistent for each molten-alloy temperature. This distance is plotted as a function of molten-alloy temperature in figure 12. As can be seen in figure 12, the downstream distance of the explosive action is a linear function of temperature for molten-alloy temperatures from 500° to 600°F. With a molten-alloy temperature of 650°F, explosions occurred at the injection-nozzle exit with no detectable smooth jet between the explosion point and the nozzle exit.

When the explosion energy reached a level at which the explosion-expanded jet diameter was 0.20 ± 0.02 inch, the overpressure that was generated was just sufficient to cause a flow stoppage. This phenomenon was consistent throughout all firing runs at all molten-alloy temperatures (that is, for all molten-alloy temperatures that were sufficiently high to cause explosion-expanded jet diameters of at least 0.20 ± 0.02). For an explosion that was energetic enough to cause an explosion-expanded jet diameter of 0.30 ± 0.05 inch, the overpressure that was generated was just sufficient to cause a backflow into the nozzle from the tank. The explosion-expanded jet diameter that was

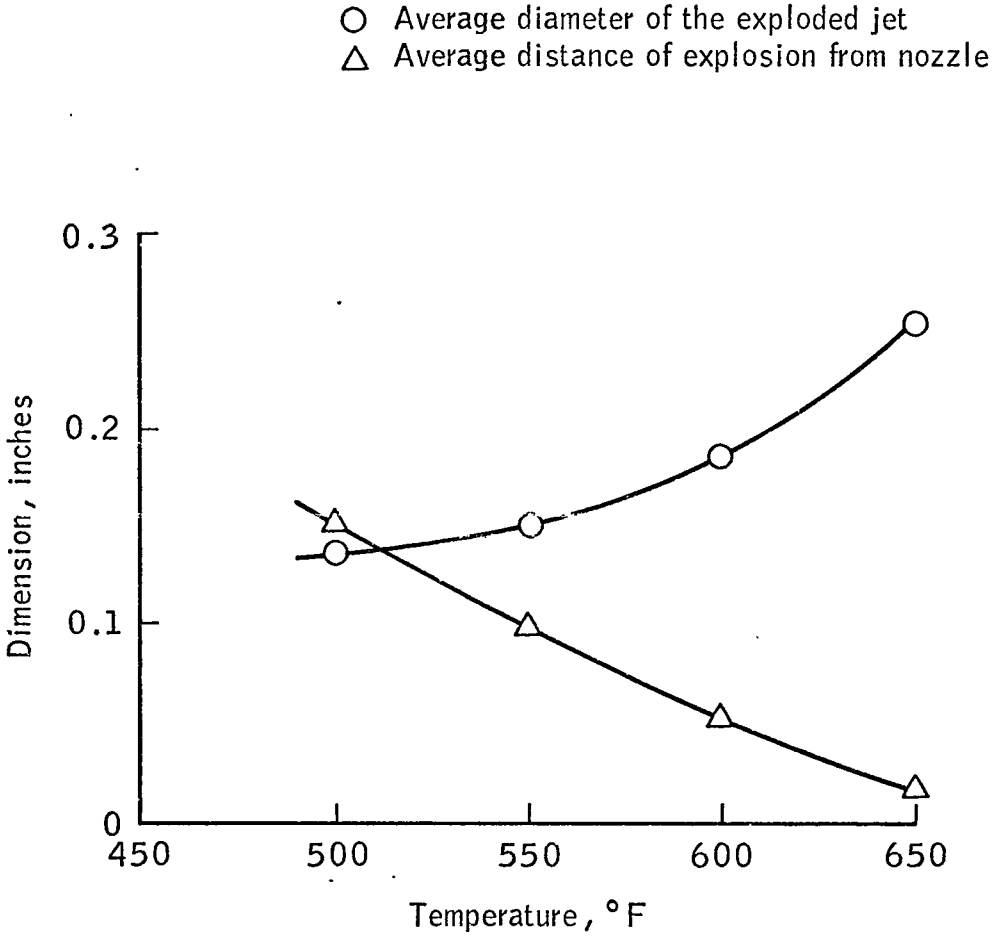

Figure 12. - Lead-Tin alloy explosion characteristics

indicative of the backflow threshold was more difficult to determine than was the jet diameter indicative of the flow-stoppage threshold. This explains the variation in accuracy between the two diameter determinations.

TIN RESULTS

A total of six operational firing runs were made with tin as the molten-metal sample. Two firing runs were made at each of three molten-metal injection temperatures, which were 550°, 600°, and 650°F. The first five firing runs were made with an injection pressure of 10 psig, and the final firing run (with a molten-tin temperature of 650°F) was made with an injection pressure of 20 psig. Several pretest firing runs were made with a molten-tin injection temperature of less than 550°F. However, at temperatures below 550°F, the jet did not start consistently because of tin solidification in the nozzle.

With the molten-tin temperature at 550°F, explosions generally occurred just as the jet emerged from the nozzle. (That is, no smooth jet segment could be observed between the end of the injection nozzle and the initial downstream explosive action.) Very few smooth jet segments were observed during the two firing runs, and when smooth segments were observed, they were always surrounded by a thick vapor layer. A total of only 10 singular or isolated explosions were observed during the two firing runs. All other explosions were continuous type explosions, and these occurred just as the molten-tin jet emerged from the injection nozzle. Both flow stoppages and backflows occurred

frequently, and each was followed by the re-emergence of the jet in the form of a spray made up of metal and vapor.

The average diameter of an explosion-expanded jet that had resulted from a singular or isolated explosion was 0.25 inch, with a diameter range of 0.20 to 0.35 inch. The downstream distance of the explosive action from the end of the nozzle was erratic and ranged from a maximum downstream distance of approximately 0.050 to a minimum distance that approached zero (that is, at the nozzle exit).

The diameter of the explosion-expanded jet that corresponded to the threshold of jet flow stoppage was 0.23 inch. All explosion-expanded jet diameters that were greater than or equal to 0.23 inch generated overpressure sufficient to at least produce flow stoppages. Explosion-expanded jet diameters of approximately 0.35 inch corresponded to the threshold for the occurrence of backflow.

In both firing runs, backflow caused premature termination of the run. In both cases, the premature termination resulted from solidification of molten tin in the injection nozzle, which prevented further flow and resulted in the remainder of the molten-tin sample being left in the pressure chamber. In the first firing run, 3.9 grams of molten tin were injected into the tank before nozzle blockage occurred, and in the second firing run, 6.9 grams were injected before blockage.

With the molten-tin temperature at 600°F, explosions were produced that resulted in overpressures greater than the 10 psig injection pressure. During both firing runs, 2 or 3 grams were injected into the quenching fluid before an explosion occurred that was energetic enough to produce backflow. However, after the first occurrence of backflow,

the jet flow became more spraylike and erratic for the remainder of the firing run, with much vapor ejected with the molten tin. Numerous small explosions of globules or particles of the spraylike jet occurred immediately after the particles were injected. A total of nine singular or isolated explosions were observed during the two firing runs.

The same flow-stoppage characteristics that had been observed in the two firing runs with a molten-tin injection temperature of 550°F were observed in the two runs with an injection temperature of 600°F. Explosion-expanded jet diameters of 0.22 inch or less did not produce overpressures sufficient ot cause flow stoppages. All explosions that produced explosion-expanded jet diameters greater than 0.22 inch produced overpressures great enough to at least cause flow stoppage. Of the nine singular explosions observed, three (which produced explosion-expanded jet diameters of 0.27, 0.30, and 0.34 inch) resulted in jet backflow. One explosion (which resulted in an explosion-expanded jet diameter of 0.24 inch) was observed to cause flow stoppage without backflow. The remaining five singular explosions (all with explosion-expanded jet diameters in the range of from 0.20 to 0.22 inch) resulted in neither backflow nor flow stoppage.

The sizes of the explosions observed during the firing runs with a molten-tin initial temperature of 600°F were not indicative of the explosion sizes expected for a 600°F sample. The discrepancy occurred because most of the singular explosions took place at the tip of the jet just as the jet emerged from the injection nozzle. This prevented a true interaction between the quenching fluid and the molten-tin jet from taking place and resulted in unpredicted explosion-expanded-jet sizes.

With the molten-tin temperature at 650°F, the explosions observed during the two firing runs (one run with an injection pressure of 10 psig and the other run with an injection pressure of 20 psig) were somewhat stronger than had been observed during the firing runs with lower molten-tin temperatures. As was the case with lower temperatures, only a few singular or isolated explosions were observed. Several explosion-expanded jet diameters did reach a maximum diameter of 0.4 inch, but most of the explosions were much smaller. As was the case during firing runs with lower molten-tin temperatures, most of the explosive action occurred at the top of the jet just as the jet emerged from the nozzle.

During the first firing run with a molten-tin temperature of 650°F and an injection pressure of 10 psig, only 2.8 grams of molten tin were injected into the quenching fluid. The abbreviated firing run was characterized by numerous short-duration flow stoppages (at almost every explosion) and several instances of backflow. After the firing run, residual particles of the molten-tin sample were recovered from the brass fitting located 12 inches above the molten-metal-jet trajectory. Propagation of sample material to this distance resulted from an explosion that produced an explosion-expanded jet diameter of 0.4 inch. This same large explosion produced extensive backflow which subsequently resulted in molten-tin solidification in the nozzle and thus, premature termination of the firing run.

To prevent solidification of molten tin in the injection nozzle and the resulting premature termination of the firing run, the second firing run with a molten-tin temperature of 650°F was conducted with an injection pressure of 20 psig. The explosion pattern was in many

ways similar to the pattern observed during the firing run with an injection pressure of 10 psig; however, several differences were noted. Rather than the explosions occurring right at the injection nozzle with no smooth jet visible between the end of the nozzle and the explosive action as had been the case for the firing runs with a 10 psig injecting pressure, with the 20 psig injection pressure, the molten-tin jet protruded 0.02 to 0.03 inch from the end of the nozzle before explosions occurred. Most of the explosions resulted in explosion-expanded jet diameters in the range of 0.25 to 0.30 inch. While explosions that produced jet diameters in this size range had been sufficent to cause jet backflow when the injection pressure was 10 psig, the overpressure produced by the explosions were insufficient to cause even flow stoppage with the higher (20 psig) injection pressure. A series of continuous explosion that produced an explosion-expanded jet diameter of 0.30 inch, however, resulted in a flow stoppage which allowed solidification of molten tin in the nozzle and premature termination of the firing run.

In summary, the explosive action that resulted from the firing runs in which molten tin was used was stronger than the explosive action for the other sample metals under the same conditions. For the firing runs in which tin was used as the sample metal, most of the explosive action occurred very near the exit of the injection nozzle, and the explosive action was generally continuous, even during the firing runs with a molten-tin temperature of 550°F. The sample residue recovered from the quenching-fluid tank after the firing runs with a molten-tin temperature of 550°F included only two or three solidified core sections

of 1 inch or more in length. The longest solidifed core section recovered was 1.75 inches long, which compared with solidified core of up to 9.5 inches recovered as the residue after firing runs under the same injection-temperature and injection-pressure conditions with the molten lead-tin alloy used as the sample metal.

Because the intensity of the explosive action (at all temperatures) was such that essentially no smooth jet segments were visible (except for the several cases when the molten-tin jet was surrounded by large concentrations of vapor), and because very few singular or isolated explosions were observed, the jet velocity was impossible to accurately measure, and the explosion-expanded jet diameters were very difficult to determine. It was also noted that because the explosive action occurred so near the nozzle exit and because most of the explosions occurred right at the tip of the jets as they emerged from the nozzle, the observed explosions were not indicative of the explosive potential of the molten tin (particularly for molten-tin temperatures of 600°F and above).

The explosions (except for the explosions that occurred during the firing run with an injection pressure of 20 psig) that produced overpressures sufficient to cause momentary flow stoppages also produced explosion-expanded jet diameters of 0.23 inch. This number must be considered to be the approximate range of explosion-expanded jet diameters that correspond to flow stoppages, since too few singular or isolated explosions were observed during the firing runs in which tin was used as the sample material. However, no case was observed in which an explosion that resulted in a jet diameter of 0.22 or

smaller caused a flow stoppage, and no case was observed in which an explosion that resulted in a jet diameter of 0.23 inch or larger did not cause at least a flow stoppage.

The increase in injection pressure from 10 psig to 20 psig for the final firing run with the molten-tin injection temperature at 650°F did not completely prevent flow stoppages, but the frequency of flow stoppages was substantially reduced. No jet backflow was observed at any time during the run. The increased injection pressure caused the explosive activity to move downstream slightly(úsually 0.02 to 0.03 inch downstream from the end of the nozzle, as opposed to explosive activity at undetectably small distances downstream for the firing runs that used a 10-psig injection pressure), although the explosive activity still generally occurred at the tip of the jet. A continuous explosion that resulted in explosion-expanded jet diameters of approximately 0.30 inch caused a flow stoppage which resulted in molten-tin solidification in the nozzle and premature termination of firing run.

The sample residue was collected from the quenching-fluid tank after each of the firing runs in which tin was used as the sample metal. Examination of the residue revealed that the inside of most of the residue particles were dark gray in color as a result of oxidation. This oxidation layer was easily scraped off, indicating a vacuum deposit of oxidized material. The outside of all the residue particles that were recovered were bright and shiny.

BOUNDARY-LAYER LOCATION

During the initial firings of the molten-metal jet it was observed that explosions were consistently occurring at a point approximately 0.10 inch downstream from the injection nozzle. It was noted that the location of the explosion point was approximately the tangency point of the boundary layer of the quenching-fluid flow (which was caused by interaction of the molten-metal jet and the water) and the molten jet. In order to test the hypothesis that the explosions were induced by circulating water coming in to close proximity with the molten-metal-jet boundary layer, a scaled drawing was made of the injection nozzle, the gate block, and the molten-metal jet. An estimated stream line was drawn by the gate block and across the injection nozzle to the point of apparent intersection with the molten metal jet as shown in figure 13. This apparent point of intersection between the streamline and the molten-metal jet was found to be very near the center of the explosions.

To further test the hypothesis that the explosions were induced by the circulating water coming in close proximity of the molten-metal jet, a thermocouple probe was constructed and mounted onto the system such that the probe extended to the location of the stream line, as predicted by the scaled drawing. A temperature traverse was then made during actual jet firing to verify the location of the stream line.

The thermocouple probe was constructed of a stainless steel tube 12 inches long with an outside diameter of 0.040 inches. The thermocouple bead was affixed in place on one end of the tube, with the bead extending 0.050 inch from the tube end. The response to the thermocouple output was recorded photographically by a camera mounted on an oscilloscope.

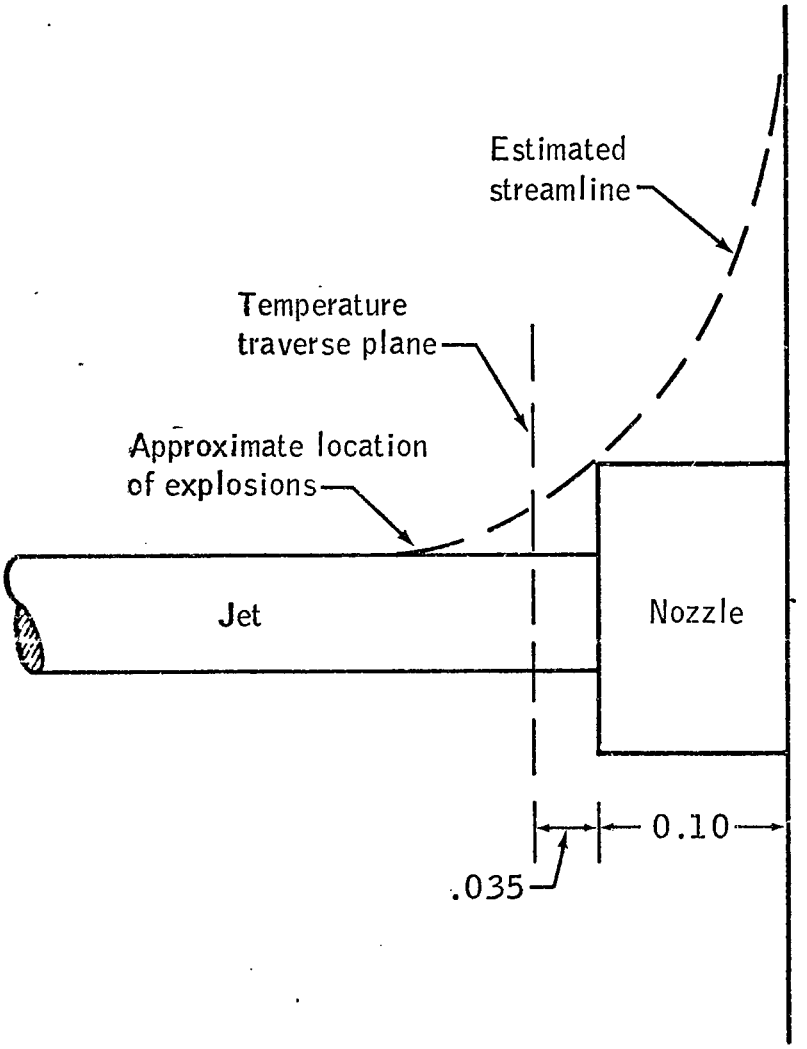

Figure 13. - Sketch of the estimated streamline and temperature traverse plane

The thermocouple probe can be seen in figure 14. The probe extends to a point just in front of and above the molten-metal injection nozzle. Also visible in figure 14 are the adjustable mountings for the probe, which enable the thermocouple on the end of the probe to be moved with respect to the molten-metal jet in the vertical plane that contains the molten-metal jet.

Operation

A total of 12 firings were made using mercury at 500° F as the working fluid. The temperature traverse to find the stream line was made along a vertical line perpendicular to the jet in the vertical plane containing the jet. The vertical traverse line was located 0.035 inch downstream from the injection nozzle exit. Measurements were made at three locations (0.025, 0.020, and 0.015 inch) above the molten-metal jet, with four jet firings at each location.

The thermocouple probe was attached to the gate block by an adjustable mount, which enabled the probe position to be easily changed. To position the probe, a stainless steel calibration rod was inserted into the injection nozzle, and the thermocouple was positioned with respect to the calibration rod with a feeler gauge. After the thermocouple had been positioned, the calibration rod was removed, the molten-metal jet was fired and the thermocouple response was recorded.

Results

When the thermocouple probe was placed 0.025 inches from the molten-metal jet, the thermocouple indicated that the temperature increased for about 0.3 second (about 10°F) and then fell slowly to near the prefiring

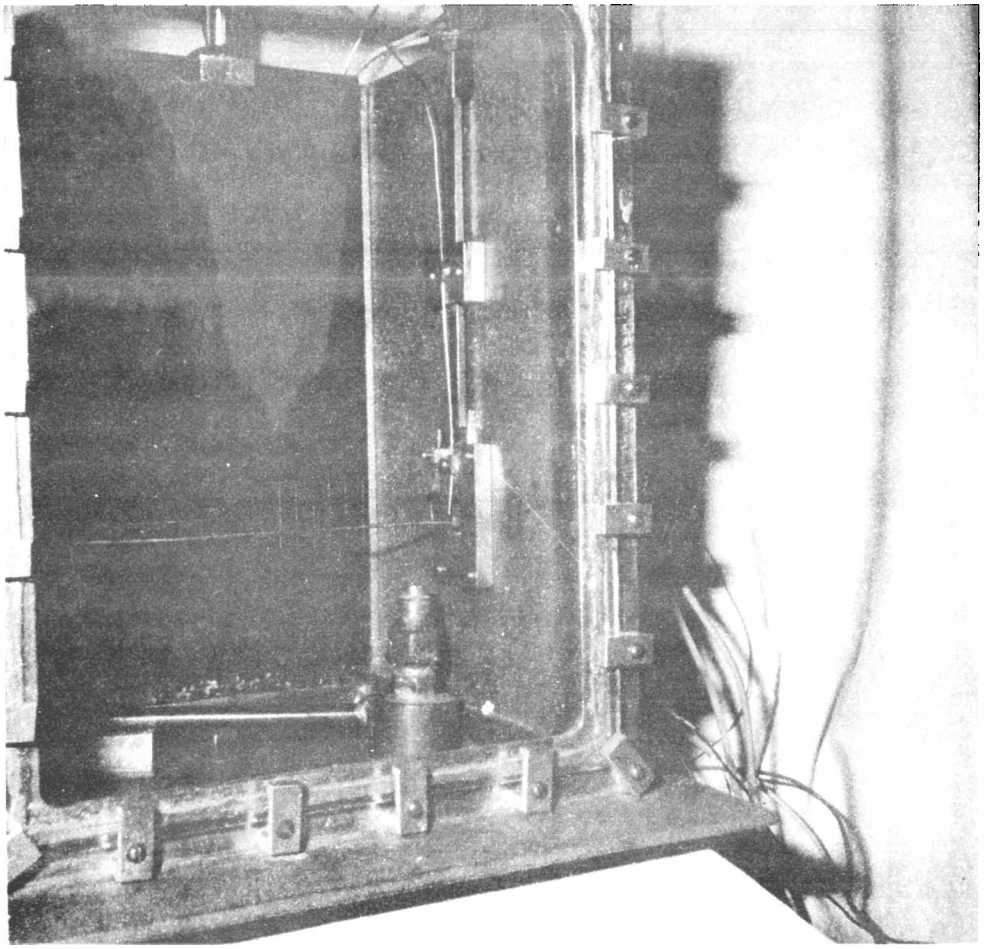

Figure 14. - Thermocouple probe mounted in the quenching-fluid tank

temperature. This pattern was characteristic of each of the four firings for this thermocouple-probe position. A typical profile of the temperature response is shown in figure 15(a).

When the thermocouple probe was placed 0.020 inch from the molten-metal jet, two of the four firings resulted in a temperature profile similar to the profile described for firing when the probe was placed 0.025 inch from the molten-metal jet. The two other firings resulted in the sudden increase, the pause, and the longer duration more gradual increase detected by the probe located 0.015 inch from the molten metal jet. A typical temperature profile for this probe position is shown in figure 15(b).

Heat from the molten-metal jet results in a temperature increase for a relatively long duration. The gradual temperature decrease observed in the four firings in which the temperature transducer was located 0.025 inch from the molten-metal jet, and in the two firings in which the transducer was located 0.020 inch from the jet was caused by the cooling effect of water circulating down the gate block along the hypothesized streamline past the temperature transducer. The lack of temperature decrease in the four firings in which the temperature transducer was located 0.015 inch from the molten-metal jet and in the two firings in which the transducer was located 0.020 inch from the jet was caused by the temperature transducer being below the streamline. At locations below the streamline no water circulates, and thus, the temperature of the transducer continues to increase.

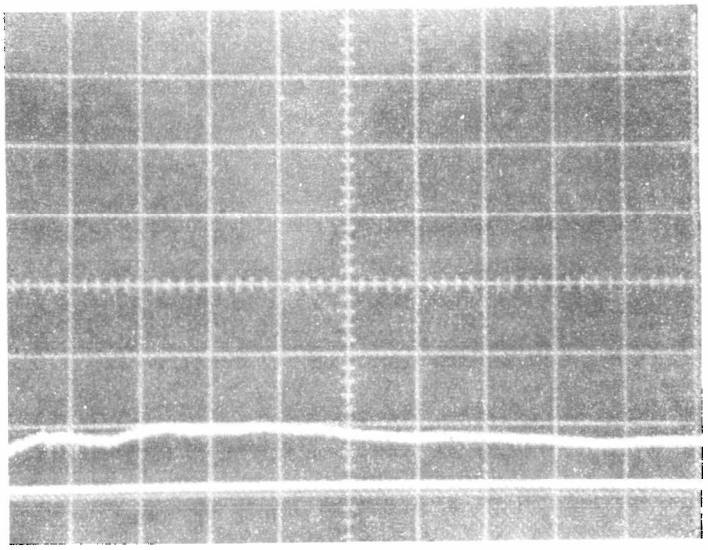

(a) Typical temperature trace with the thermocouple positioned above the streamline

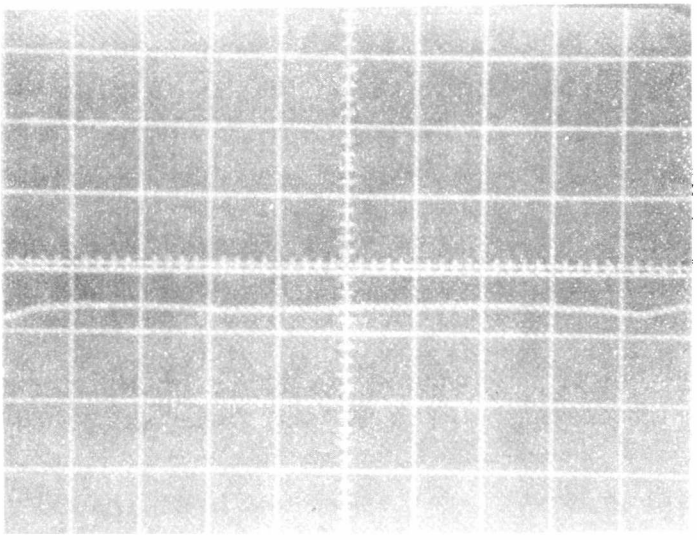

(b) Typical temperature trace with the thermocouple positioned below the streamline

Figure 15. - Thermocouple response to boundary-layer traverse

Conclusion

The determination was made that the streamline was located 0.020 inch above the molten-metal jet at a point 0.035 inch from the nozzle exit. This had been almost exactly the predicted location of the streamline. Thus, the hypothesis that the explosions observed during the initial firings of the molten-metal jet had been caused by the close proximity of the streamline with the boundary layer of the molten-metal jet was shown to be correct.

SURFACE-COOLING EFFECT

After some of the experimental results had been reviewed, it became apparent that the explosions of the molten-metal jet were very sensitive to the circulation of the cooler quenching fluid into the proximity of the molten-metal jet surface. The explosive reaction of the jet to the cooler water was so rapid that it appeared to have been a surface-cooling phenomenon that had triggered the explosion. Also, other investigators have found an explosion threshold at higher temperatures than were observed in the experiments described in this report. For these reasons an experimental check was made of surface cooling of a molten-metal jet.

The check was made by making a new gate and nozzle for the molten-metal-jet injector out of yellow brass. The nozzle and gate that had been used in the operational test runs had been made of stainless steel. Yellow brass has a higher thermal diffusivity than stainless steel, and thus, will cool the surface of the molten-metal jet more efficiently

than will stainless steel. The total time that any cross section of the molten-metal jet remains in the nozzle is less than 3 milliseconds. Thus, only the material very near the surface of the molten-metal jet would be influenced by the temperature of the nozzle.

Two test firings of the lead-tin alloy with the yellow brass nozzle were made with the molten metal at 600°F and under a pressure of 10 psig. The resulting residue was compared with the residue obtained from the firing under the same conditions when the stainless steel nozzle was used. The results are shown in figure 16. The residue using the brass nozzle is the long core on the right.

The tendency for the molten-metal jet to explode was considerably less when the yellow brass nozzle was used. When the stainless steel nozzle was used, explosions frequently occurred that tore the molten-metal jet apart and even caused stoppages and back flow in the nozzle. The residues resulting from both test firings in which the brass nozzle was used were continuous cores of solidifed metal 14 inches long. That is, the explosions had not been violent enough to tear the molten-metal jet apart. The cores were highly porous and were approximately 0.2 inch in diameter. The explosions were relatively gentle, which caused the high porosity cores to have a "popcorn" appearance. No stoppages or back flow were observed at the nozzle during either test firing with the brass nozzle.

It can thus be concluded that explosion intensity is highly sensitive to surface cooling of the molten-metal jet. The explosion potential decreases as the surface temperature of the molten-metal jet decreases.

Figure 16. - Residue comparison between the stainless steel nozzle and the brass nozzle

7. DISCUSSION OF EXPERIMENTAL RESULTS

AVERAGE HEAT TRANSFER RATE

Solidification of the jet

The average heat-transfer rate was determined for the firing runs in which the molten lead-tin alloy at a temperature of 500°F was used as the injected sample. A 500°F injection temperature was chosen because lower injection temperatures resulted in frequent lead-tin alloy solidification in the nozzle, which caused jet flow blockage. Higher injection temperatures were not used because of the increased explosive activity at higher temperatures inhibited the desired smooth solidification of the jet. The calculation of the average heat transfer rate was made by first determining the downstream distance of the jet solidification point from the end of the injection nozzle. This solidification point was for segments of the jet that were undisturbed by explosive action from the time they left the nozzle until they reached the downstream point where they solidified. The solidification point was determined to be consistent at approximately 0.63 inch downstream from the exit of the nozzle.

As the jet moved downstream through the quenching fluid, the jet would become somewhat distorted and would bend slightly. Of course, after solidification of the jet had occurred, the bending movement and distortion would cease. Thus, the solidification point could be found by determining the point at which jet distortion stopped, and

this point could be determined by a careful examination of the movie film of the firing run. The solidification point was most easily found by running the film backward and locating the point at which motion first appeared.

The time required for a point on a smooth segment of jet to travel from the end of the nozzle downstream to the solidification point was measured. The average heating rate was then calculated by use of the equation

$$q'' = \frac{(h_s + h_f)\,\dot{m}}{\dot{A}\,\Delta T}$$

where $\dot{m}$ is the mass flow rate, h_s is the sensible heat loss, h_f is the heat of fusion, and $\dot{A}$ is the area rate of jet extrusion. The heating rate thus calculated was found to be 8.4×10^6 Btu/hr-ft^2. This value for the heating rate corresponds to an average heat transfer coefficient of 2.91×10^4 Btu/hr-ft^2-°F, if $T_{initial} - T_{saturation}$ is used as the driving-temperature difference. A "ball park" type comparison was made between the heating rate calculated for the molten-alloy jet and the heating rates for a copper sphere, obtained by Stevens [6]. The single data point calcualted previously is shown plotted on Stevens' graph (fig. 17) and appears to be reasonable. The velocity of the molten-alloy jet (8.2 ft/sec) was lower than the velocity of the copper sphere (9.5 ft/sec), and the thermal diffusivity for copper is higher than the thermal diffusivity for the lead-tin alloy. However, these factors were compensated for by (1) the greater agitation of the molten jet as compared with a solid sphere,

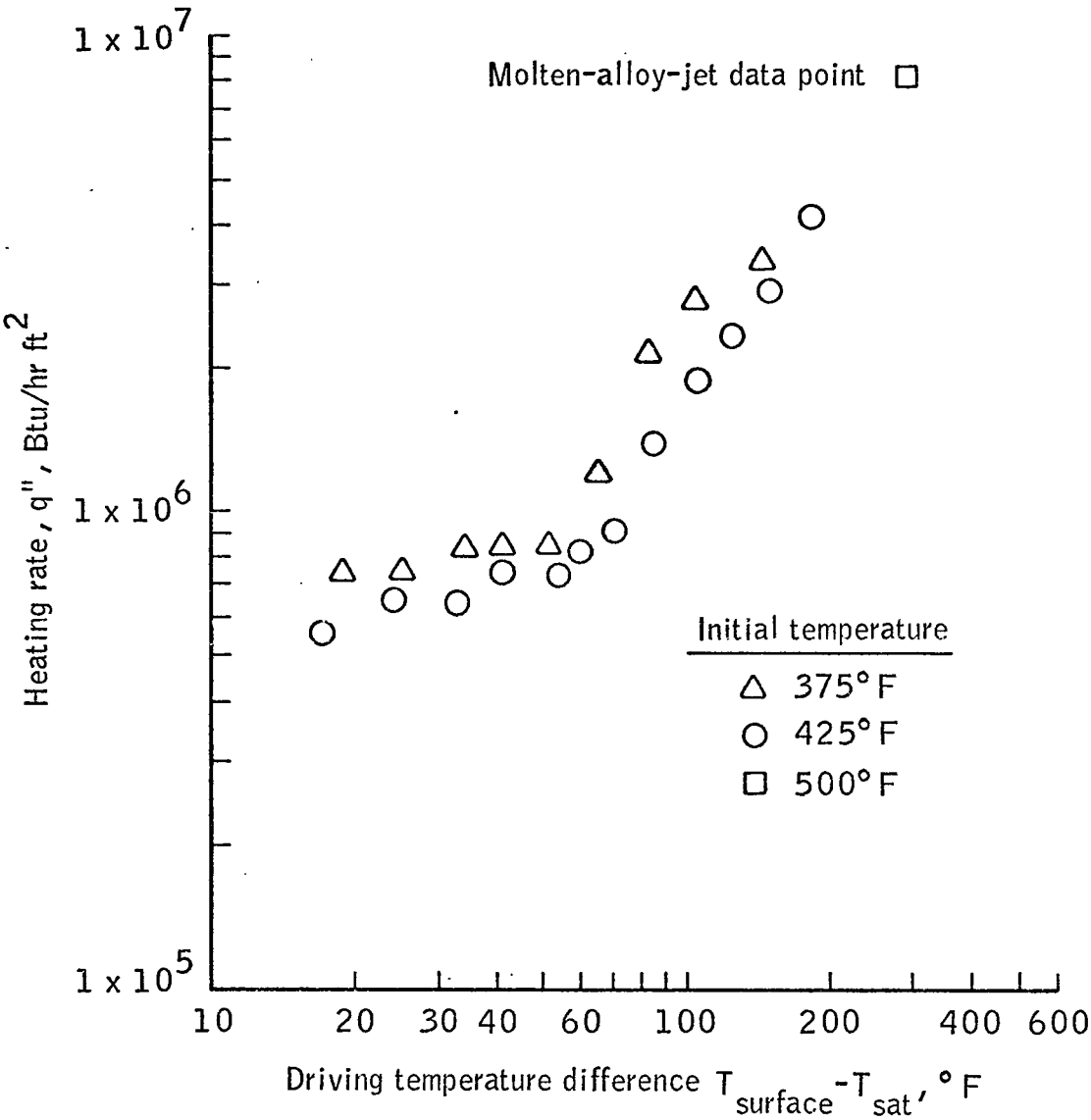

Figure 17. - Heating rate as a function of driving temperature difference

(2) the thermal diffusivity for the molten-alloy jet is considerably higher (50 percent or more) than for a solid-alloy jet, and (3) the driving-temperature difference for the molten-alloy jet is slightly higher than the driving temperature difference for the solid copper sphere.

The stability of the solidification-point location indicates an error-function-shaped temperature profile, as derived by Simon [7]. Otherwise, for a more common parabolic-type temperature profile, such as for a suddenly cooled cylinder, the downstream distance of the solidification point from the end of the nozzle would be expected to fluctuate.

Solidification of Explosion Debris

A jet that expands as a result of an explosion solidifies almost instantaneously after the explosion. For firing runs with a relatively low molten-alloy temperature (500° to 550°F), the explosion duration is 0.20 to 0.50 millisecond. For these low-temperature explosions that are not violent enough to cause disintegration of the molten-alloy jet, the end of an explosion is marked by the termination of jet expansion, and this termination of jet expansion is a result of jet solidification. Since the solidification time of a free molten-alloy jet was determined to be 6.4 milliseconds, the solidification time for a jet that is expanding as a result of an explosion is smaller by a factor of approximately 20.

Solidification of an explosion-expanding jet in 0.50 millisecond or less is not necessarily unreasonable. The estimated area increase between an explosion-expanded jet of Asarcolo 158 with an injection temperature of 600°F and an unexpanded jet of Asarcolo 158 (discussed later in this dissertation) was greater than 1000 percent. The lead-tin alloy jet area increase is considerably greater than 1000 percent, as can be seen by a visual comparison of the residue of the samples. In addition, the heat-transfer rate closer to the injection nozzle is greater than the average heat-transfer rate (in the vicinity of the streamline apparent intersection with the molten-metal jet which is discussed in the section entitled "Boundary-Layer Location"). The factor of 20 reduction in solidification time between a normal free molten-alloy jet and an explosion-expanding molten-alloy jet is understandable if consideration is given to both the area increase of an explosion-expanded jet over an unexpanded jet and the increase in the heat-transfer rate that results from the boundary-layer disturbances from the outward radial velocity of the jet during an explosion.

SYSTEM PARAMETER ANALYSIS

An effort was made to use dimensional analysis to determine the important parameters of the explosion phenomenon. However, data were not readily available for the molten metal tested to enable a correlation of the dimensional-analysis results with the experimental results.

The explosive action should be related to some dimensionless number (or modulus) that is derived from the following:

1. Material properties
2. Thermodynamic variables of the system
3. Dynamic variables of the system

The derived number should have the following characteristics.

1. It is normally finite.
2. It has a minimum positive value at or above which an explosion will occur.
3. It is valid for a liquid (or nonsolidified) sample.
4. Its magnitude should increase with an increase in explosive potential.
5. It should be related in magnitude to the magnitude of the explosive action.

In table I are listed the necessary parameters to be used in the dimensional analysis.

Dimensionless Group Derivation

The dimensionless group is assumed to be a function of all the variables listed in table I.

$$B = B\ (h_f,\ C_p,\ k,\ \rho,\ \sigma,\ D,\ \theta,\ h,\ K,\ \beta) \qquad (1)$$

Thus

$$B = \left(\frac{B}{m}\right)^a \left(\frac{B}{mT}\right)^b \left(\frac{B}{\gamma LT}\right)^c \left(\frac{m}{L^3}\right)^d \left(\frac{m}{\gamma^2}\right)^c (L)^f (T)^g \left(\frac{B}{\gamma L^2 T}\right)^h \left(\frac{m}{\gamma^2 L}\right)^i \left(\frac{1}{T}\right)^j \qquad (2)$$

TABLE I. - NECESSARY PARAMETERS FOR THE DIMENSIONAL ANALYSIS

PARAMETER	SYMBOL	UNITS	DIMENSION
Fusion heat $h_f = h_f + C_p \Delta T$ $\Delta T = T - T_{solid}$	h_f	B/lb_m	B/M
Specific heat	C_p	$B/lb_m\ °F$	B/MT
Thermal conductivity	K	B/hr ft °F	$B/\gamma LT$
Density	ρ	lb_m/ft^3	M/L^3
Surface tension, $\sigma = \sigma g_c$	σ	$\frac{lb_f}{ft} g_c$	M/γ^2
Characteristic length	D	ft	L
Characteristic temperature, $\theta = T - T_{quench}$	θ	°F	T
Heat transfer coefficient	h	$B/hr\ ft^2\ °F$	$B/\gamma L^2 T$
Bulk Modulus	K	$g_c\ lb_f/ft^2$	$M/\gamma^2 L$
Coefficient of thermal expansion	β	$\frac{ft}{ft}/°F$	$\frac{1}{T}$

The sum of the exponents of each parameter must sum to zero for the number or the variable group to be dimensionless. Thus, we can write

$$\begin{aligned} &\text{Energy, B:} && 0 = a + b + c + h \\ &\text{Mass, M:} && 0 = -a - b + d + e + i \\ &\text{Temp., T:} && 0 = -b - c + g - h - j \\ &\text{Time, } \gamma\text{:} && 0 = -c - 2e - h - 2i \\ &\text{Length, L:} && 0 = -c - 3d + f - 2h - i \end{aligned} \tag{3}$$

If equations (3) are solved in terms of a, b, c, f, and j, then

$$h = -a - b - c \tag{4}$$

$$g = -a + j \tag{5}$$

$$e = -c - f \tag{6}$$

$$i = (a + b)/2 + c + f \tag{7}$$

$$d = (a + b)/2 \tag{8}$$

If equations (4) to (8) are substituted into equation (2), along with the variables given in equation (1)

$$\begin{aligned} B = (h_f)^a\ (C_p)^b\ (k)^c\ (\rho)^{\frac{a}{2}\frac{b}{2}}\ (\sigma)^{-c-f}\ (D)^f\ (\theta)^{-a+j} \\ (h)^{-a-b-c}\ (K)^{\frac{a}{2}+\frac{b}{2}+c+f}\ (\beta)^j \end{aligned} \tag{9}$$

By collecting terms with like exponents

$$B = \left[\frac{h_f\ \rho^{\frac{1}{2}}\ K^{\frac{1}{2}}}{\theta h}\right]^a \left[\frac{C_p\ \rho^{\frac{1}{2}}\ K^{\frac{1}{2}}}{h}\right]^b \left[\frac{kK}{\sigma h}\right]^c \left[\frac{DK}{\sigma}\right]^f \left[\theta\beta\right]^j \tag{10}$$

Now, if a = b and c = f

$$B = \left[\frac{h_f DK}{\alpha\theta h}\right]^a \left[\frac{DK}{\sigma}\right]^{2c} \left[\frac{k}{hD}\right]^{c+a} \left[\theta\beta\right]^j \tag{11}$$

if $c = -a$

$$B = \left[\frac{\alpha\theta hDK}{h_f\sigma^2}\right]^{-a} \left[\theta\beta\right]^{j} \tag{12}$$

If $j = -a$

$$B = \frac{\alpha\theta^2 hDK\beta}{h_f\sigma^2} \tag{13}$$

Dimensionless Group Qualitative Assessment

The terms θ and h_f vary proportionally with the absolute temperature. They represent the driving temperature difference and the sensible (or latent) energy absorbing parameter, respectively, of the metal sample. For the lead-tin alloy, the ratio of the two parameters was calculated for various temperatures, and the results are shown in table II.

As can be seen from table II, the ratio of the driving temperature difference and the effective fusion heat is fairly constant over a wide range of temperatures. Thus, the combination of the two parameters should have little effect on the explosion causative mechanism. The terms D and K are constant, and α is nearly constant for a given system.

An explanation for the explosion causative phenomenon, then, should lie with the four remaining variables, which are θ, β, h, and σ. These variables appear in the form $\theta h\beta/\sigma^2$, which is the heating rate (q) times the ratio of sample contraction and the square of the

TABLE II. - VARIATION OF THE RATIO OF θ/h_f WITH TEMPERATURE

Temperature, °F	θ/h_f, $\frac{°F\ lb}{Btu}$
400	23.5
500	23.8
600	24.0
700	24.1
800	24.2
900	24.3
1000	24.4
1500	24.6
2000	24.7

sample surface tension β/σ^2. Both parameters (q and β/σ^2) are strong functions of temperature. The heating rate increases as the temperature increases; and β generally increases and σ decreases with increasing temperature.

The hypothesis is proposed that the causative mechanism is a surface phenomenon and that the parameter controlling both the explosion threshold and the explosion magnitude for a given system is the product of the heating rate and the ratio of the sample linear thermal expansion and the sample surface tension. This hypothesis is supported by the following experimental observations.

1. The explosive action is highly sensitive to the sample surface temperature, to a much greater extent than to the sample bulk temperature. This was shown by the substitution of the brass nozzle for the stainless steel nozzle.

2. The explosion threshold and explosion magnitude are different for different materials.

3. Explosions occur more readily when the liquid/vapor interface approaches the molten-metal sample. This was observed on numerous occasions throughout the experiments.

4. The work by Flory, Paoli, and Mesler [8] showed that the fragmentation and dispersion of the sample increased greatly with decreased sample surface tension.

More generally, it is postulated that both the lower limit of the explosion threshold and the magnitude of the resulting explosions are directly related to the dimensionless group of parameters. The lower

limit explosion threshold for a given sample and system should correspond to a particular constant value of the dimensionless group.

RESIDUE PARTICLE ANALYSIS OF ASARCOLO 158

The samples of the Asarcolo 158 tests were analyzed. This is the only sample material that was amenable to this type of analysis due to the highly irregular shape of the residue of both the tin and the lead-tin alloy.

Particle Size Distribution

Five recovered samples were screened to determine the particle size distribution. One sample each at five different temperatures was picked at random for the screening. The larger size particles (0.065 inch and larger) were very irregular in shape and often consisted of two or more particles fused together. The smaller particles were more regularly shaped, with a high percentage being relatively spherical, ellipsoidal or flat. The screens used were hand-shaker type standard sieve series of the following sizes: 0.0025, 0.0035, 0.0138, 0.0469, and 0.065 inch.

It should be noted that not all of the sample was recovered from the tank after each run. In all cases, 16 grams were loaded into the pressure chamber. After the run, the system was checked carefully to ensure that no material was left in the chamber. Each run left a high concentration of small particles suspended in the water, and some floating on top of the water. The suspended particles were easily visible in the water.

The particle size distribution, as determined with the screens, is shown in figure 18 for each temperature. The particle size is progressively smaller with increased injection temperature.

In figure 19, the same screening data are plotted in the same way except for the assumption that all of the non-recovered metal was suspended in the water and had a 0.0035-inch dimension or smaller. This assumption is subject to error in that some of the material may have been physically lost, but this is not too bad since reasonable care was taken to collect all of the sample residue after each run.

The largest screen size used was 0.065 inch as stated previously. Although a relatively high percent by weight of the material was greater than 0.065 inch dimension, the actual particle count was low. The particle count and percentage by weight of the two larger screen sizes are shown in table III.

The results of the particle size distribution are not wholly due to explosive action. Each sample contained argon bubbles near the end of the run that caused breakup to the jet and some sample scatter.

Area Estimate

The final surface area of the sample residue was estimated. The technique used was to use the particle sizes shown in figure 19 at the mid-point between two screen sizes, and then assume that all of the screened particles within that range were spheres of the mid-point diameter. From the known weight of material at that diameter and the metal density, the number of particles were estimated and from this the surface area of representative spheres was calculated.

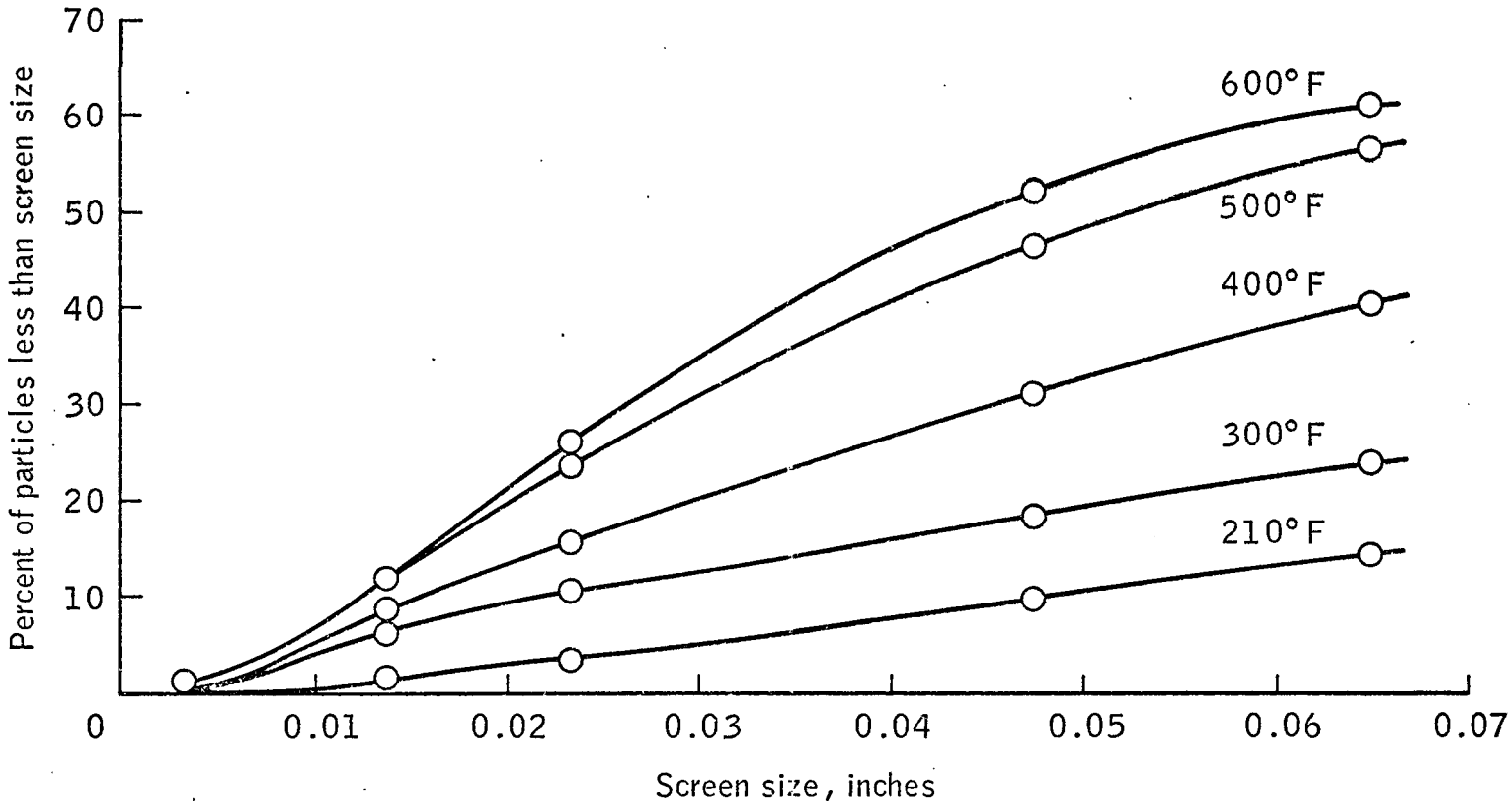

Figure 18. - Particle size distribution, as screened

TABLE III. - COUNT OF PARTICLES RETAINED IN TOP TWO SCREENS

PARTICLES RETAINED IN SCREEN	TEMPERATURE, °F				
	210	300	400	500	600
0.065 screen count	70	66	69	56	63
Percent by weight	77.5	71.9	56.9	40.8	34.1
0.0469 screen count	40	36	64	84	65
Percent by weight	4.1	5.0	8.6	10.2	7.3

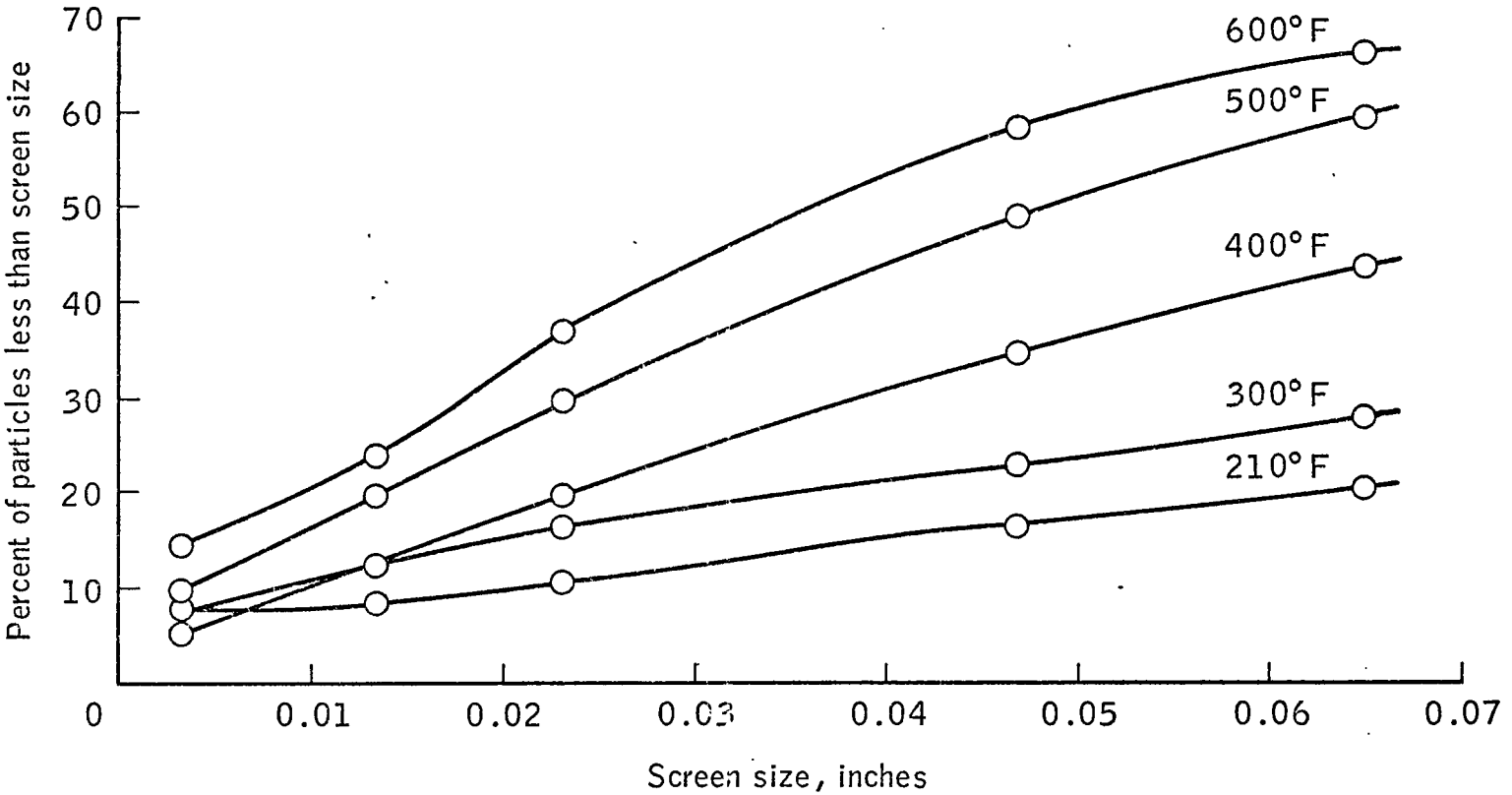

Figure 19. - Particle size distribution assuming nonrecovered particles were 0.0035 inches or smaller

For particles greater in size than 0.065 inch, the actual particle counts shown in table III were used to calculate the surface area of equivalent spheres of the same average weight. This estimate is conservative since the particles were not round and the surface area of ellipsoidal or flat particle would be greater than the estimate. The area estimates for the large particle (above 0.065 inch screen size) are shown in table IV, and range from 3.70 in^2 at 210°F to 2.07 in^2 at 600°F.

Table V shows the small-particle area estimates for each mid-point diameter used. The total area estimates of these particles ranged from 29.58 in^2 at 210°F to 68.40 in^2 at 600°F.

The total area estimate and percentage increase of area of the exploded jet is shown in table VI. The increase in area ranged from 500% to 1050%.

Jet Disturbance

One run of Asarcolo 158 at 300°F and 2 psig ejection pressure was made just out of curiosity. The average velocity of the jet was 28 inches per second.

Vertical bands of low light reflections were visible on this jet and the jet broke up about 0.5 inch from the nozzle into solid near-spherical particles. The separation of the jet at breakup always occurred at one of the dark bands. Indeed the bands were seen to be circumferential depressions in the jet.

TABLE IV. - LARGE PARTICLE AREA ESTIMATES

	TEMPERATURE, °F				
	210	300	400	500	600
Particle count	70	66	69	56	63
Weight, grams	12.4	11.5	9.1	6.5	5.5
Area, in^2	3.70	3.46	3.01	2.25	2.07

TABLE V. - SMALL-PARTICLE AREA ESTIMATES

PARTICLES		TEMPERATURE, °F				
		210	300	400	500	600
$D^{(a)} = .056$	Weight, gm.	0.66	0.8	1.38	1.63	1.17
	Area, in^2	.46	.56	.96	1.14	.82
D = .0351	Weight	0.95	1.10	2.35	2.95	3.60
	Area	1.05	1.22	2.61	3.28	4.00
D = .0185	Weight	0.41	0.60	1.17	1.68	2.00
	Area	.87	1.26	2.46	3.54	4.22
D = .0087	Weight	0.10	0.90	1.20	1.70	1.42
	Area	.45	4.03	5.38	7.63	6.36
D = .00175	Weight	1.2	1.08	0.81	1.52	2.38
	Area	26.75	24.05	18.05	33.90	53.00
Total Area, in^2		29.58	31.12	29.46	49.49	68.40

(a) D is the particle diameter in inches

TABLE VI. - TOTAL PARTICLE SURFACE AREA INCREASE

	TEMPERATURE, °F				
	210	300	400	500	600
Total area, in^2	33.3	34.6	32.5	51.7	70.5
Area increase, percent	500	520	488	775	1050

Due to this observation, the number of the bands per inch were counted on all of the lower temperature jets. Above 400°F the jets were obscured by vapor, particles, and explosions to the extent that a count was not feasible. The number of bands per 0.25 inch was consistent within each run. The data is shown in table VII.

The same type of data for the lead-tin alloy are shown in table VIII. Three runs at 500°F are shown. The distance from the nozzle to the first disturbance is also shown.

TABLE VII. - BAND COUNT PER 0.25 INCH OF JET FOR ASARCOLO 158

TEMPERATURE, °F							
	210	210	300[a]	300	300	400	400
	16[b]	14	5	10	11	15	10
	15	14	6	10	10	10	15
	14	13	5	11	10	12	13
	17	16	6	14	11	14	15
	18	15	6	9	9	14	12
	13	16	5	11	8	12	16
	17	17	4	10	10	12	10
	15	20	7	13	10	15	13
	14	16	5	12	10	11	14
	14	16	6	11	10	12	12
	16	14	5	11	10	12	13
	14	15	4	10	11	13	10
Avg.	15.3	15.5	5.3	11.0	10.3	12.7	12.6
Avg. Vel.	81	N/A	28	78	86	81	94

(a) Two pounds per square inch injection pressure.

(b) All numbers in the table are band counts per 0.25 inch.

TABLE VIII. - BAND COUNT PER 0.25 INCH OF JET FOR LEAD-TIN ALLOY AT 500°F

	First run		Second run		Third run	
	Count	Distance,[a] in.	Count	Distance, in.	Count	Distance, in.
	10	0.11	8	0.04	12	0.02
	10	0.12	9	0.04	11	0.06
	8	0.08	10	0.08	12	0.09
	10	0.11	8	0.05	8	0.07
	9	0.13	9	0.04	10	0.10
	9	0.10	7	0.06	12	0.05
Avg.	9.3	0.11	8.5	0.05	10.9	0.07
Vel. in/sec	85		95		103	

(a) Distance from nozzle to first disturbance

8. CONCLUSIONS AND RECOMMENDATIONS

Several significant results were obtained from this investigation.

1. A non-solidifying jet of mercury will explode.

2. Explosions can (and did) occur below the boiling point of water.

3. The size of the exploded jet is a function of sample temperature.

4. The overpressure generated by an explosion is a function of the exploded jet size and sample material.

5. Explosions occur when the vapor layer is thin or collapsed.

6. The distance of the explosion from the nozzle exit plane is a function of injection temperature.

7. The explosive action is highly sensitive to the sample surface temperature - much more so than to the sample bulk temperature.

This experimental investigation using a molten-metal jet has provided valuable insights into the causative mechanism of the vapor explosion phenomena. In particular, it has been shown that the published theories of the causative mechanism are in fact incorrect. The mechanisms proposed by the published theories may indeed be contributors, but they are not necessary to trigger a vapor explosion. In fact, in its elemental form, the vapor explosion has been shown to be not a vapor explosion at all, since the explosion can (and did) occur below the temperature where vapor is formed. It is suggested that the so-called vapor explosion phenomena would more correctly be labeled a "thermal shock explosion", since the evidence suggests that thermal

shock is the causative mechanism of the explosion, and vapor formation is merely a contributor to the magnitude of violence of the overall action.

The "thermal shock explosion" theory was proposed to this investigator by Dr. L. C. Witte*. This theory states that the thermal shock causes a compression wave that travels to the center of the molten metal sample,then propagates outward as an expansion wave. This expansion wave causes fragmentation of the sample and the subsequent explosion. The initial compression wave is caused by the combined forces from surface tension and linear thermal contraction.

The thermal shock theory is supported by the following evidence.

1. The explosions occur when the surrounding liquid comes into close proximity of the molten sample, facilitating a high heat transfer rate.

2. Fragmentation is necessary for high-energy explosions.

3. The tin samples were oxidized on the inside, indicating an out-bound expansion wave with a corresponding vacuum region at the sample center.

4. Dimensional analysis results indicate that the controlling parameters may be heat transfer rate, surface tension, and linear thermal expansion. These three surface parameters are necessary and sufficient to cause the hypothesized thermal shock wave.

5. The experiments of Flory et al [8] have shown that surface tension is a key parameter.

---

* Mechanical Engineering Department, University of Houston

6. The explosive potential is very sensitive to surface temperature.

The following recommendations are offered for additional investigations.

1. Studies should be conducted to determine the effects of both surface tension and linear thermal expansion.

2. Studies should be conducted to determine the quantity and rate of energy release. These studies should include pressure, surface temperature, and surface area determination.

3. A comprehensive dimensional analysis should be conducted and correlated with experimental and analytical results.

4. Additional investigations should be made similar to those described herein using different metals, temperatures, injection velocities, and jet diameters.

REFERENCES

1. Witte, L. C., Cox, J. E., and Bouvier, J. E., "The Vapor Explosion," Journal of Metals; Vol. 22, No. 2, Feb. 1970.

2. Epstein, L. F., "Analytical Formulation for the Reaction Rate," Metal Water Reactions, Vol. 6, Sept. 1959.

3. Higgins, H. M., "The Reaction of Molten Uranium and Zirconium Alloys with Water," Aeroject General Report No. Agc-AE-7, Apr. 1965.

4. Miller, R. W., Spano, A. H., Dugone, J., Wieland, D. D., and Houghtaling, J. E., "Experimental Results and Damage Effects of Destructive Test," Transactions of the American Nuclear Society, Vol. 6, 1963.

5. American Smelting and Refining Company, "Asarcolo Fusible Alloys," Bulletin 1, No. 13, July 1962.

6. Stevens, J. W. and Witte, L. C., "Transient Film and Transition Boiling from a Sphere," International Journal of Heat and Mass Transfer (to be published).

7. Simon, W. E., "Analysis of the Heat Transfer Characteristics of an Emergent Jet," Ph. D. Dissertation, University of Houston, 1970.

8. Flory, K., Paoli, R., and Mesler, R., "Molten Metal-Water Explosions," Chemical Engineer Progress, Vol. 65, Dec. 1969.